

# A STABLE FAST TIME-STEPPING METHOD FOR FRACTIONAL INTEGRAL AND DERIVATIVE OPERATORS \*

FANHAI ZENG<sup>†</sup>, IAN TURNER<sup>†,‡</sup>, AND KEVIN BURRAGE<sup>†,§</sup>

**Abstract.** In this work, we propose a stable fast time-stepping method for both fractional integral and derivative operators. The fractional operator is decomposed into a local part with memory length  $\Delta T$  and a history part, where the local part is approximated by the direct convolution method and the history part is approximated by a fast memory-saving method. The current fast method has  $O(n_0 + \kappa(N) \log(n_T - n_0))$  active memory and  $O(n_0 n_T + \kappa(N)(n_T - n_0) \log(n_T - n_0))$  operations, where  $n_0 = \Delta T/\tau$ ,  $n_T = T/\tau$ ,  $\tau$  is the stepsize,  $T$  is the final time, and  $\kappa(N)$  is the number of quadrature points in the truncated Gauss–Laguerre quadrature used in the fast method. We present numerical examples and compare with the known methods to verify the effectiveness of the fast method.

**Key words.** Fast convolution, the (truncated) Gauss–Laguerre quadrature, short memory principle, fractional differential equations, fractional Lorenz system.

**AMS subject classifications.** 26A33, 65M06, 65M12, 65M15, 35R11

**1. Introduction.** The convolution of the form

$$\int_0^t k(t-s)u(s) \, ds \quad (1.1)$$

arises in many physical models, such as integral equations, integrodifferential equations, fractional differential equations, and classical integer-order differential equations such as the wave propagation with nonreflecting boundary conditions, see for example, [7, 24, 26, 30, 20]. The direct discretization of (1.1) takes the form

$$\sum_{k=0}^n \omega_{n-k} u(t_k), \quad n = 1, 2, \dots, n_T, \quad (1.2)$$

where  $\omega_n$  are the convolution quadrature weights. The direct computation of (1.2) requires  $O(n_T)$  active memory and  $O(n_T^2)$  operations, which is expensive for long time computations. The computational difficulty in both memory requirement and computational cost will increase greatly when the direct approximation (1.2) is applied to resolve high-dimensional time evolution equations and/or a large system of time-fractional partial differential equations (PDEs) involving (1.1), see e.g., [36, 41].

The aim of this paper is to present a stable and fast memory-saving time-stepping algorithm for the convolution (1.1) with a kernel  $k(t) = t^{\alpha-1}/\Gamma(\alpha)$ . When  $\alpha \geq 0$ , Eq. (1.1) gives a fractional integral of order  $\alpha$ . If  $\alpha < 0$ , then Eq. (1.1) can be interpreted as the Hadamard finite part integral, which is equivalent to the Riemann–Liouville (RL) fractional derivative of order  $-\alpha$  (see Lemma 2.5).

In the last decade, fractional models have been widely applied due to their applications in science and engineering, see [7, 24, 26]. There have been many numerical

---

\*This work was supported by ARC Discovery Project DP150103675

<sup>†</sup>School of Mathematical Sciences, Queensland University of Technology, Brisbane, QLD 4001, Australia (f2.zeng@qut.edu.au).

<sup>‡</sup>Australian Research Council Centre of Excellence for Mathematical and Statistical Frontiers, Queensland University of Technology, Brisbane, QLD 4001, Australia (i.turner@qut.edu.au)

<sup>§</sup>Visiting Professor, Department of Computer Science, University of Oxford, OX1 3QD, UK (kevin.burrage@qut.edu.au)

methods for discretizing fractional operators and resolving fractional differential equations (FDEs), see [7, 15, 26]. However, the nonlocality of fractional operators leads to much more expensive computational cost and memory requirement of the majority of numerical methods for FDEs, see [10, 14]. However, this computational difficulty has not been well solved. The short memory principle (see [5, 26]) seems promising to resolve this difficulty, but it has not been widely applied in fractional calculus due to its inaccuracy.

Up to now, there have been only a few numerical works on reducing storage requirements and computational cost for solving nonlocal models. Lubich and Schädle [20] proposed a fast convolution method for the convolution (1.1), in which the kernel  $k(t)$  was first expressed by its inverse Laplace transform, then the trapezoidal rule was applied to discretize the inverse Laplace transform. This idea was then extended to calculate the discrete convolution (1.2) in [28]. The adaptive stepsize version given in [20] was developed in [18] and an application of [20] in the simulation of fractional-order viscoelasticity in complicated arterial geometries was proposed in [36]. The storage and computational cost of the fast convolutions in [18, 20, 28] are  $O(\log n_T)$  and  $O(n_T \log n_T)$ , respectively, which are much less than the direct methods with  $O(n_T)$  memory and  $O(n_T^2)$  operations.

For the fractional integral operator of order  $\alpha \in [0, 1)$ , the corresponding kernel  $k_\alpha(t) = t^{\alpha-1}/\Gamma(\alpha)$  can also be expressed by

$$k_\alpha(t) = \frac{1}{\Gamma(\alpha)\Gamma(1-\alpha)} \int_0^\infty \lambda^{-\alpha} e^{-\lambda t} d\lambda.$$

Then the Gauss–Legendre quadrature was applied to approximate the above integral in [16]. The method presented in [16] was extended in [14] to approximate the Caputo fractional derivative operator of order  $0 < \alpha < 1$  with a slight modification, in which both the Gauss–Jacobi and Gauss–Legendre quadratures were utilized. In [23], McLean proposed a method to approximate the fractional integral by use of a degenerate kernel to approximate the fractional kernel  $k_\alpha(t)$ , which leads to a fast time-stepping method with  $O(M \log n_T)$  active memory and  $O(M n_T \log n_T)$  operations. Recently, Baffet and Hesthaven [1] have proposed a kernel compression method to discretize the fractional integral operator. Their method is based on multipole approximation to the Laplace transform of the kernel  $k_\alpha(t)$ . In [25], a fast numerical contour integral method for linear space-fractional diffusion equations was developed. Here, we mainly focus on fast time-stepping methods for the evolution equations, numerical methods for space-fractional differential equations are not discussed, readers can refer to [13, 33, 32, 43] for more information.

In this work, we follow and generalize the approach in [20], while we apply Henrici's formula [4] to express the kernel  $k_\alpha(t)$  in the fractional operator, which is approximated by the (truncated) Gauss–Laguerre quadrature. Thanks to the Hadamard finite part integral, the RL fractional derivative can be approximated in the same way as the fractional integral. This idea was also adopted in [40] to develop three-term recurrence formulas to calculate the fractional integral and derivative of the weighted Jacobi polynomials; see also [6, 17].

We need only focus on a fast and memory-saving algorithm for the fractional integral (1.1) with  $k(t) = t^{\alpha-1}/\Gamma(\alpha)$ ,  $\alpha \in [0, 1)$ , as the derived algorithm then can be extended to approximate the fractional derivative operator of any order without any modification. A slight modification can be made to discretize the fractional integral of order  $\alpha \in [1, 2)$ .

We list the main contributions of this work as follows.

- In Section 3, we follow the idea in [20] to present our memory-saving fast convolution method for approximating both the fractional integral and derivative operators. We apply the (truncated) Gauss–Laguerre quadrature to approximate the kernels in the fractional integral and derivative operators instead of the trapezoidal rule used in [20]. Since all the Gauss–Laguerre quadrature points are positive, we solve a series of stable ordinary differential equations (ODEs) of the form  $y'(t) = -\lambda y(t) + u(t)$ , where  $\lambda > 0$  is a Gauss–Laguerre quadrature point, see (3.10). In the fast convolution given in [20],  $\lambda$  is a complex number, which may have a negative real part that may affect the stability of the method in [20], see (3.18). We compare our fast method with that proposed in [20], and show that the present method may have smaller round off errors, see Figures 3.1 and 3.2.
- Since the solutions to the FDEs are generally nonsmooth [7], we introduce correction terms to deal with non-smooth solutions, hence highly accurate numerical solutions are obtained, see Section 4.
- The short memory principle with lag-terms is resolved with high accuracy and low computational cost in Section 5. This can be seen as a generalization of the fast method in Section 3. By choosing suitable parameters, our method can be simplified as that in [16, 14], where the time domain does not need to be divided into exponentially increasing intervals, which simplifies the implementation of the algorithm; see numerical results shown in Figure 7.1, and also Figure 6.1.
- A guideline on how to choose the basis  $B$  ( $B > 1$  is a positive integer, see (3.7)) used in the fast convolution is provided and verified, see (6.8) and numerical verifications in Tables 6.4–6.5. Compared with the fast method in [20], we can increase  $N$  such that a relatively larger basis  $B$  can be applied in applications, see results shown in Table 6.4.

We also present sufficient numerical simulations to verify the accuracy of the present fast convolution, and the comparison with the direct method is also made to show the high efficiency of the current fast method.

We would like to emphasize that the *truncated* Gauss–Laguerre quadrature is applied in the present fast method, which reduces the memory and computational cost significantly, see  $\kappa(N)$  in Table 6.3. The memory and computational cost in [20, 18] can be halved due to the symmetry of the trapezoidal rule, but operations with complex numbers are involved. In addition, the Gauss–Jacobi and Gauss–Legendre quadrature used in [16, 14] may not be truncated. Furthermore, the discretization error caused from the Gauss–Laguerre quadrature is independent of the stepsize and the regularity of the solution to the considered FDE, and is also not sensitive to the fractional order  $\alpha \in [-2, 1]$ .

This paper is organized as follows. In Section 2, we introduce the definitions of the fractional integral and derivative operators. Then we follow the approach in [20] to present our fast method in Section 3. In Section 4, the correction terms are introduced in the fast method to deal with nonsmooth solutions of FDEs. A generalization of the fast method in Section 3 is developed in Section 5 and a criteria on choosing the basis  $B$  is investigated in Section 6. We present sufficient numerical experiments to verify the present fast method in Section 7 before the conclusion in the last section.

**2. Preliminaries.** In this section, we introduce the relevant definitions of the fractional integral and derivative, and the properties that will be used in this work.

DEFINITION 2.1 (RL fractional integral). *The RL fractional integral operator  $D_{0,t}^{-\alpha}$  of order  $\alpha$  ( $\alpha \geq 0$ ) is defined by*

$$D_{0,t}^{-\alpha} u(t) = {}_{RL}D_{0,t}^{-\alpha} u(t) = \frac{1}{\Gamma(\alpha)} \int_0^t (t-s)^{\alpha-1} u(s) ds. \quad (2.1)$$

DEFINITION 2.2 (RL fractional derivative). *The RL fractional derivative operator  ${}_{RL}D_{0,t}^{\alpha}$  of order  $\alpha$  is defined by*

$${}_{RL}D_{0,t}^{\alpha} u(t) = \frac{1}{\Gamma(n-\alpha)} \frac{d^n}{dt^n} \int_0^t (t-s)^{n-\alpha-1} u(s) ds, \quad (2.2)$$

where  $n-1 < \alpha \leq n$ ,  $n$  is a positive integer.

DEFINITION 2.3 (Caputo fractional derivative). *The Caputo fractional derivative operator  ${}_C D_{0,t}^{\alpha}$  of order  $\alpha$  is defined by*

$${}_C D_{0,t}^{\alpha} u(t) = \frac{1}{\Gamma(n-\alpha)} \int_0^t (t-s)^{n-\alpha-1} \frac{d^n}{ds^n} u(s) ds, \quad (2.3)$$

where  $n-1 < \alpha \leq n$ ,  $n$  is a positive integer.

Next, we introduce the Hadamard finite part integral, which plays crucial roles in the numerical approximation of the RL fractional derivative operator.

DEFINITION 2.4 (Hadamard finite part integral, see [27]). *Let a function  $f(x)$  be integrated on an interval  $(\epsilon, A)$  for any  $A > 0$  and  $0 < \epsilon < A$ . The function  $f(x)$  is said to possess the Hadamard property at the point  $x = 0$  if there exist constants  $a_k, b_0$  and  $\lambda_k > 0$  such that*

$$\int_{\epsilon}^A f(x) dx = \sum_{k=1}^N a_k \epsilon^{-\lambda_k} + b_0 \ln \frac{1}{\epsilon} + J_0(\epsilon), \quad (2.4)$$

where  $\lim_{\epsilon \rightarrow 0} J_0(\epsilon)$  exists and is finite, which is also denoted by

$$\mathfrak{f}_0^A f(x) dx = \lim_{\epsilon \rightarrow 0} J_0(\epsilon). \quad (2.5)$$

Using the above definition of the finite part integral, we obtain the following property.

LEMMA 2.5 (see [27, p. 112]). *The RL fractional derivative  ${}_{RL}D_{0,t}^{\alpha} u(t)$ ,  $\alpha > 0, \alpha \neq 1, 2, \dots$ , is equivalent to the following integral in the Hadamard sense, that is*

$${}_{RL}D_{0,t}^{\alpha} u(t) = \frac{1}{\Gamma(-\alpha)} \mathfrak{f}_0^t (t-s)^{-\alpha-1} u(s) ds. \quad (2.6)$$

**3. A stable fast convolution.** In this section, we follow the approach given in [20] to develop our fast convolution and compare it with that in [20].

Let  $K(\lambda)$  be the Laplace transform of  $k(t)$ . Then the inverse Laplace transform of  $K(\lambda)$  is given by  $k(t) = \frac{1}{2\pi i} \int_{\Gamma} K(\lambda) e^{t\lambda} d\lambda$ , where  $\Gamma$  is a suitable complex contour.  $\frac{1}{2\pi i} \int_{\Gamma} K(\lambda) e^{t\lambda} d\lambda$  can be exponentially approximated by the trapezoidal rule, namely

$$k(t) = \frac{1}{2\pi i} \int_{\Gamma} K(\lambda) e^{t\lambda} d\lambda \approx \sum_{j=-N}^N \omega_j K(\lambda_j) e^{t\lambda_j} \quad (3.1)$$

with a suitably chosen complex contour  $\Gamma$ , such as the Talbot contour (see [20, 34]), the parabolic contour (see [35]), and the hyperbolic contour (see [25, 35]). The trapezoidal rule (3.1) was used to develop a fast convolution to approximate a convolution of the type (see [18, 20, 28]),

$$\int_0^t k(t-s)u(s) \, ds. \quad (3.2)$$

In this work, we do not use the trapezoidal rule (3.1). Instead, we will use Henrici's formula (see [4]), which gives

$$k(t) = \frac{1}{2\pi i} \int_0^\infty [K(\lambda e^{-i\pi}) - K(\lambda e^{i\pi})] e^{-t\lambda} \, d\lambda$$

to express the inverse Laplace transform of the kernel  $k(t)$ , then the Gauss–Laguerre quadrature is applied to approximate the above integral. In the following, we denote  $k_\alpha(t)$  and its Laplace transform  $K_\alpha(\lambda)$  as follows

$$k_\alpha(t) = t^{\alpha-1}/\Gamma(\alpha), \quad K(\lambda) = \lambda^{-\alpha}. \quad (3.3)$$

Inserting  $K_\alpha(\lambda) = \lambda^{-\alpha}$  into Henrici's formula, we have

$$k_\alpha(t) = \frac{1}{\Gamma(\alpha)\Gamma(1-\alpha)} \int_0^\infty \lambda^{-\alpha} e^{-t\lambda} \, d\lambda = \frac{\sin(\alpha\pi)}{\pi} \int_0^\infty \lambda^{-\alpha} e^{-t\lambda} \, d\lambda. \quad (3.4)$$

Our goal is to discretize the right-hand side of (3.4) using a highly accurate numerical method. We naturally think of Gauss–Laguerre quadrature. Specifically, we have the following approximation

$$k_\alpha(t) = \frac{\sin(\alpha\pi)}{\pi} \int_0^\infty \lambda^{-\alpha} e^{-T\lambda} e^{-(t-T)\lambda} \, d\lambda \approx \frac{\sin(\alpha\pi)}{\pi} \sum_{j=0}^N \omega_j e^{-(t-T)\lambda_j}, \quad (3.5)$$

where we choose a suitable  $T$  such that  $0 < T \leq t$ ,  $\{\omega_j\}$  and  $\{\lambda_j\}$  are the Gauss–Laguerre quadrature weights and points that correspond to the weight function  $\lambda^{-\alpha} e^{-T\lambda}$ . ■

Denote  $t_n = n\tau$  ( $n = 0, 1, \dots, n_T$ ) as the grid point, where  $\tau$  is the stepsize. We first restrict ourselves to  $\alpha \in [0, 1)$ . Using (3.5) and following the idea in [20], we present our stable fast convolution for approximating  $\int_0^t k_\alpha(t-s)u(s) \, ds$  as follows:

- Step 1) Decompose the convolution  $\int_0^t k_\alpha(t-s)u(s) \, ds$  as

$$\begin{aligned} \int_0^t k_\alpha(t-s)u(s) \, ds &= \int_{t-\tau}^t k_\alpha(t-s)u(s) \, ds + \int_0^{t-\tau} k_\alpha(t-s)u(s) \, ds \\ &\equiv L^\alpha(u, t) + H^\alpha(u, t), \end{aligned} \quad (3.6)$$

where we call  $L^\alpha(u, t)$  and  $H^\alpha(u, t)$  the local and history parts, respectively.

- Step 2) For every  $t = t_n$ , let  $L$  be the smallest integer satisfying  $t_n < 2B^L\tau$ , where  $B > 1$  is a positive integer. For  $\ell = 1, 2, \dots, L-1$ , determine the integer  $q_\ell$  such that

$$s_\ell = q_\ell B^\ell \tau \quad \text{satisfies} \quad t_n - s_\ell \in [B^\ell \tau, (2B^\ell - 1)\tau]. \quad (3.7)$$

Set  $s_0 = t_n - \tau$  and  $s_L = 0$ . Then  $t_n - \tau = s_0 > s_1 > \dots > s_{L-1} > s_L = 0$ . Moreover,  $s_\ell$  is uniquely determined for any fixed  $t = t_n$ .

- Step 3) Using (3.5), we approximate the history part  $H^\alpha(u, t)$  by

$$\begin{aligned}
H^\alpha(u, t_n) &= \frac{\sin(\alpha\pi)}{\pi} \sum_{\ell=1}^L \int_0^\infty \lambda^{-\alpha} e^{-T_{\ell-1}\lambda} e^{-(t_n - s_{\ell-1} - T_{\ell-1})\lambda} y(s_{\ell-1}, s_\ell, \lambda) d\lambda \\
&\approx \frac{\sin(\alpha\pi)}{\pi} \sum_{\ell=1}^L \sum_{j=0}^N \omega_j^{(\ell)} e^{-(t_n - s_{\ell-1} - T_{\ell-1})\lambda_j^{(\ell)}} y(s_{\ell-1}, s_\ell, \lambda_j^{(\ell)}) = H_\tau^{(\alpha, n)} u
\end{aligned} \tag{3.8}$$

with  $y(s_{\ell-1}, s_\ell, \lambda)$  given by

$$y(s_{\ell-1}, s_\ell, \lambda) = \int_{s_\ell}^{s_{\ell-1}} e^{(s-s_{\ell-1})\lambda} u(s) ds, \tag{3.9}$$

where  $\{\omega_j^{(\ell)}\}$  and  $\{\lambda_j^{(\ell)}\}$  are the Gauss–Laguerre quadrature weights and points that corresponds to the weight function  $\lambda^{-\alpha} e^{-T_{\ell-1}\lambda}$ , and  $T_{\ell-1}$  is independent of  $t_n$  that satisfies  $t_n - s - T_{\ell-1} \geq 0$  for all  $t_n - s \in [B^{\ell-1}\tau, (2B^\ell - 1)\tau]$ ,  $s \in [s_\ell, s_{\ell-1}]$ . Here  $y(s) = y(s, s_\ell, \lambda_j^{(\ell)})$  used in (3.8) that is defined by (3.9) satisfies the following ODE

$$y'(s) = -\lambda_j^{(\ell)} y(s) + u(s), \quad y(s_\ell) = 0. \tag{3.10}$$

Obviously, all  $\lambda_j^{(\ell)}$ 's in the linear ODE (3.10) are positive, and (3.10) can be well solved by the following recursive relation

$$y(t_{n+1}) = e^{-\lambda_j^{(\ell)}\tau} y(t_n) + e^{-\lambda_j^{(\ell)}\tau} \int_{t_n}^{t_{n+1}} e^{\lambda_j^{(\ell)}(s-t_n)} u(s) ds.$$

The above relation is inconvenient to implement in real computations. However, we can replace  $u$  with its interpolation  $I_\tau^{(p,n)}u$ , where  $I_\tau^{(p,n)}(n \geq p-1)$  is the  $p$ th-order interpolation operator that corresponds to the points  $\{t_{n-p+1}, t_{n-p+2}, \dots, t_{n+1}\}$ , that is

$$\begin{aligned}
I_\tau^{(p,n)} u(t) &= \sum_{j=0}^p u(t_{n-p+1+j}) l_j^{(p,n)}(t), \\
l_j^{(p,n)}(t) &= \prod_{k=0, k \neq j}^p \frac{t - t_{n-p+1+k}}{t_{n-p+1+j} - t_{n-p+1+k}}.
\end{aligned} \tag{3.11}$$

If  $n \leq p-1$ , then we let  $I_\tau^{(p,n)}u(t) = I_\tau^{(p,p-1)}u(t)$ . Let  $y_n$  be the approximate solution of  $y(t_n)$ , then  $y(t_{n+1})$  can be approximated by the following numerical scheme

$$\begin{aligned}
y_{n+1} &= e^{-\lambda_j^{(\ell)}\tau} y_n + e^{-\lambda_j^{(\ell)}\tau} \int_{t_n}^{t_{n+1}} e^{\lambda_j^{(\ell)}(s-t_n)} I_\tau^{(p,n)} u(s) ds \\
&= e^{-\lambda_j^{(\ell)}\tau} y_n + \sum_{k=0}^p \psi_k^{(p)} u(t_{n+1-k}), \quad n \geq p-1.
\end{aligned} \tag{3.12}$$

Theoretically,  $\psi_k^{(p)}$  in (3.12) can be calculated exactly. In this paper, we will apply quadratic interpolation in the numerical simulations. Let  $p = 2$  in (3.12), we have

$$y_{n+1} = e^{-\lambda_j^{(\ell)}\tau} y_n + \psi_2^{(2)} u_{n-2} + \psi_1^{(2)} u_{n-1} + \psi_0^{(2)} u_n, \tag{3.13}$$

where

$$\begin{aligned}\psi_0^{(2)} &= \frac{1}{2\lambda_j^{(\ell)}} \frac{1}{(\lambda_j^{(\ell)}\tau)^2} \left[ (2 - \lambda_j^{(\ell)}\tau)e^{\lambda_j^{(\ell)}\tau} - 2 - \lambda_j^{(\ell)}\tau \right], \\ \psi_1^{(2)} &= -\frac{1}{\lambda_j^{(\ell)}} \frac{1}{(\lambda_j^{(\ell)}\tau)^2} \left[ (2 - (\lambda_j^{(\ell)}\tau)^2)e^{\lambda_j^{(\ell)}\tau} - 2 - 2\lambda_j^{(\ell)}\tau \right], \\ \psi_2^{(2)} &= \frac{1}{2\lambda_j^{(\ell)}} \frac{1}{(\lambda_j^{(\ell)}\tau)^2} \left[ (2 + \lambda_j^{(\ell)}\tau)e^{\lambda_j^{(\ell)}\tau} - 2 - 3\lambda_j^{(\ell)}\tau - 2(\lambda_j^{(\ell)}\tau)^2 \right].\end{aligned}\quad (3.14)$$

- Step 4) For the local part  $L^\alpha(u, t_n) = \int_{t_n-\tau}^{t_n} k_\alpha(t_n - s)u(s) ds$ , we replace  $u$  with its interpolation  $I_\tau^{(p,n)}u$ , which leads to

$$L^\alpha(u, t_n) \approx L(I_\tau^{(p,n)}u, t_n) = \sum_{k=0}^p \phi_k^{(p)} u_{n-k} = L_\tau^{(\alpha,n,p)}u, \quad (3.15)$$

where the  $\{\phi_k^{(p)}\}$  can be calculated exactly. For  $p = 2$ , we have

$$\phi_2^{(2)} = \frac{-\alpha\tau^\alpha}{2\Gamma(3+\alpha)}, \quad \phi_1^{(2)} = \frac{\alpha(3+\alpha)\tau^\alpha}{\Gamma(3+\alpha)}, \quad \phi_0^{(2)} = \frac{(4+\alpha)\tau^\alpha}{2\Gamma(3+\alpha)}. \quad (3.16)$$

Combining Steps 1)–4), we obtain our fast convolution for approximating  $\int_0^t k_\alpha(t-s)u(s) ds$ . The above fast convolution has the same storage and computational cost as that in [20], the main difference is listed below:

- i) Gauss–Laguerre quadrature is applied instead of the trapezoidal rule to approximate the history part  $H^\alpha(u, t) = \int_0^{t-\tau} k_\alpha(t-s)u(s) ds$ , that is, the history part  $H^\alpha(u, t)$  in [20] was approximated by

$$H^\alpha(u, t_n) \approx \text{Im} \left\{ \sum_{\ell=1}^L \sum_{j=-N}^N \hat{\omega}_j^{(\ell)} K(\hat{\lambda}_j^{(\ell)}) e^{(t_n-s_{\ell-1})\hat{\lambda}_j^{(\ell)}} \hat{y}(s_{\ell-1}, s_\ell, \hat{\lambda}_j^{(\ell)}) \right\} = \hat{H}_\tau^{(\alpha,n)}u, \quad (3.17)$$

where  $\{\hat{\omega}_j^{(\ell)}\}$  and  $\{\hat{\lambda}_j^{(\ell)}\}$  are the weights and quadrature points for the Talbot contour  $\Gamma_\ell$ , and  $\hat{y}(s) = \hat{y}(s, s_\ell, \hat{\lambda}_j^{(\ell)}) = \int_{s_\ell}^s e^{-(s-s_{\ell-1})\hat{\lambda}_j^{(\ell)}} u(s) ds$  satisfies the following ODE

$$\hat{y}'(s) = \hat{\lambda}_j^{(\ell)} \hat{y}(s) + u(s), \quad y(s_\ell) = 0. \quad (3.18)$$

- ii) We solve a stable ODE (3.10) instead of a possibly unstable ODE (3.18) that may affect the stability and accuracy of (3.17). Indeed, for the Talbot contour used in [20] (see also the parabolic contour or hyperbolic contour discussed in [35]), there exist  $\hat{\lambda}_j^{(\ell)}$ 's, whose real parts are positive. Numerical tests show that (3.17) still works well since one may not solve (3.18) for a long time, which reduces the iteration error from solving (3.18) even though the real part of some  $\hat{\lambda}_j^{(\ell)}$  is positive.

As a direct result of Lemma 2.5, the above fast convolution Step 1) – Step 4) can be used to approximate the fractional derivative operator of any order, that is, the fractional derivative operator of order  $-\alpha$  is thus discretized if  $\alpha < 0$ .

Next, we discuss how to choose  $T_{\ell-1}$  such that (3.8) preserves exponential accuracy. In Step 3), it is reasonable to choose  $T_{\ell-1}$  in order that  $t_n - s - T_{\ell-1} \geq 0$  for all  $t_n - s \in [B^{\ell-1}\tau, (2B^\ell - 1)\tau]$ ,  $s \in [s_\ell, s_{\ell-1}]$ . Therefore, a simple choice of  $T_{\ell-1}$  can be  $T_{\ell-1} = B^{\ell-1}\tau$ . If  $T_{\ell-1} > B^{\ell-1}\tau$ , then  $t_n - s - T_{\ell-1} < 0$  for some  $s \in [s_\ell, s_{\ell-1}]$ , thus  $e^{-(t_n-s_{\ell-1}-T_{\ell-1})\lambda} \rightarrow \infty$  as  $\lambda \rightarrow \infty$  for some  $\ell$ , which should be avoided in real computations.

In the following, we focus on the discretization error of (3.8) caused by the Gauss–Laguerre quadrature. To this end, we can set  $u(s) = 1 + s$ , so that  $y(s_{\ell-1}, s_\ell, \lambda_j^{(\ell)})$  in (3.8) (see also (3.9)) can be calculated exactly, i.e.,

$$y(s_{\ell-1}, s_\ell, \lambda_j^{(\ell)}) = \frac{1}{\lambda_j^{(\ell)}} \left[ \left( 1 - \frac{1}{\lambda_j^{(\ell)}} \right) \left( 1 - e^{-\lambda_j^{(\ell)}(s_{\ell-1}-s_\ell)} \right) + s_{\ell-1} - s_\ell e^{-\lambda_j^{(\ell)}(s_{\ell-1}-s_\ell)} \right] \quad (3.19)$$

EXAMPLE 3.1. Let  $u(s) = 1 + s$  in (3.8) and define the relative error

$$e^{(m)}(t_n) = \frac{|H^\alpha(u, t_n) - H_\tau^{(\alpha, n)} u|}{|H^\alpha(u, t_n)|}, \quad m = 1, 2, \quad (3.20)$$

where  $H_\tau^{(\alpha, n)} u$  is defined by (3.8). For  $m = 1$ ,  $y(s_{\ell-1}, s_\ell, \lambda_j^{(\ell)})$  in  $H_\tau^{(\alpha, n)} u$  is given by (3.19) (Exact ODE solver); for  $m = 2$ ,  $y(s_{\ell-1}, s_\ell, \lambda_j^{(\ell)})$  in  $H_\tau^{(\alpha, n)} u$  is obtained by solving ODE (3.10) via the recurrence relation (3.12) (Recurrence ODE solver).

We choose  $u(s) = 1 + s$  in order that the error  $e^{(1)}$  mainly comes from the Gauss–Laguerre quadrature, and the error  $e^{(2)}$  comes from both the Gauss–Laguerre quadrature and the iteration error caused by the numerical method (3.12) for solving ODE (3.10). We compare the errors  $e^{(1)}$  and  $e^{(2)}$  for different  $\alpha$ , which are shown in Figures 3.1(a) and (b). We can see that  $e^{(1)}$  is smaller than  $e^{(2)}$ , since the recurrence ODE solver has large round off errors when  $\tau$  is small and/or  $\lambda_1^{(\ell)} = \min_{0 \leq j \leq N} \{\lambda_j^{(\ell)}\}$  is small. It is easy to derive that  $\lambda_j^{(\ell)} / \lambda_j^{(\ell+1)} = B$ , which means that the minimum quadrature point  $\lambda_1^{(\ell)}$  decreases as  $\ell$  increases. For example, for  $\alpha = -0.8$ , we have  $\lambda_1^{(\ell)} \approx 1.2532 \times 10^{-3}, 2.5063 \times 10^{-4}, 5.0126 \times 10^{-5}, 1.0025 \times 10^{-5}$  for  $\ell = 7, 8, 9, 10$ , respectively. If we increase the stepsize  $\tau$ , i.e.,  $\tau = 0.1, 1$ , then the error  $e^{(2)}$  from the recurrence ODE solver becomes smaller, and  $e^{(1)}$  and  $e^{(2)}$  are almost identical for  $\tau = 1$ , see Figure 3.1(b). Therefore, we conclude that our method shows stable behavior in real computations.

We present in Figure 3.2 the corresponding errors  $e^{(1)}$  and  $e^{(2)}$  in [20], see (3.17). We can see that satisfactory numerical results are also obtained, but the present fast convolution (see red curve in Figure 3.1) shows better accuracy.

**4. Fast convolution with correction terms.** Generally speaking, solutions of FDEs are non-smooth, they may have strong singularity. The non-smoothness of the solution  $u(t)$  to the considered FDE may yield a less accurate numerical solution  $y_{n+1}$  of  $y(t_{n+1})$ . Therefore, the local part  $L^\alpha(u, t_n)$  is also not well approximated when  $u(t)$  is non-smooth.

In order to approximate the local part and the history part accurately, we follow Lubich's correction method [19]. We first consider the approximation of the local part

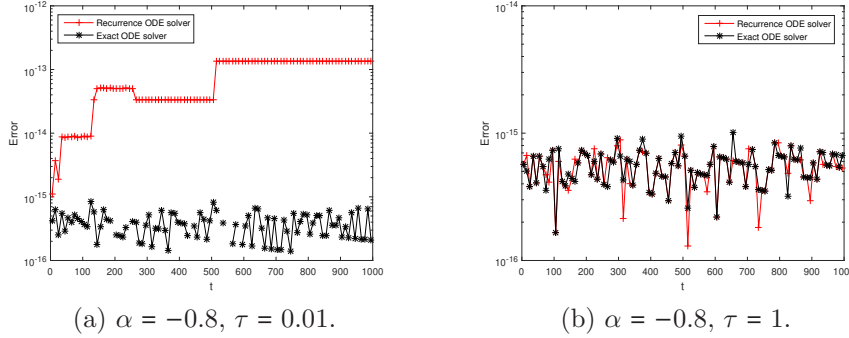


FIG. 3.1. Comparison between the exact ODE solver (black curve) and the recurrence ODE solver (red curve),  $B = 5, N = 80$ .

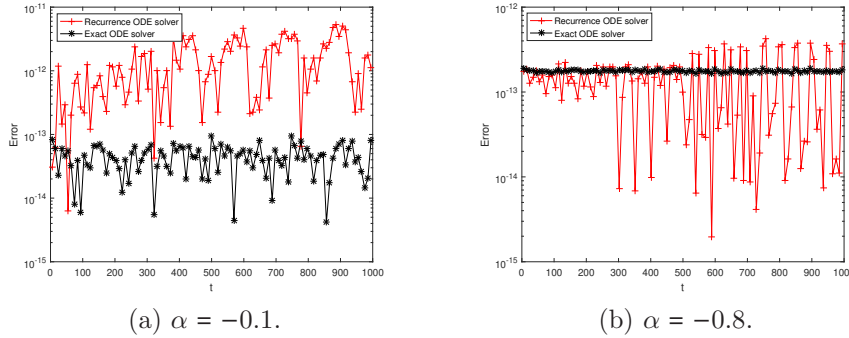


FIG. 3.2. Comparison between the exact ODE solver (black curve) and the recurrence ODE solver (red curve),  $\tau = 0.01, B = 5, N = 32$ . The optimal contour  $z(\theta, N) = N(-0.4814 + 0.6443(\theta \cot(\theta) + i0.5653\theta))$  obtained in [34] is applied here, i.e.,  $\hat{\lambda}_j^{(\ell)}$  in (3.17) is given by  $\hat{\lambda}_j^{(\ell)} = z(\theta_j, N/(2T_{\ell-1} - \tau))$  with the corresponding weight  $\hat{\omega}_j^{(\ell)} = \partial_\theta z(\theta_j, N/(2T_{\ell-1} - \tau))$ , where  $\theta_j = (2j + 1)\pi/(2N), j = -N, \dots, N - 1$  and  $T_\ell = B^\ell \tau$ .

$L^\alpha(u, t_n)$  with correction terms, which is given by

$$L^\alpha(u, t_n) \approx \sum_{k=0}^p \phi_k^{(p)} u_{n-k} + \sum_{j=1}^{q_1} w_{n,j}^{(1)} (u_j - u_0) = L_\tau^{(\alpha, n, p, q_1)} u, \quad (4.1)$$

where the starting weights  $\{w_{n,j}^{(1)}\}$  are chosen such that Eq. (4.1) is exact for some  $u(t) = t^{\sigma_k}$  ( $k = 1, 2, \dots, q_1$ ). Specifically, for quadratic interpolation, the starting weights  $\{w_{n,j}^{(1)}\}$  can be determined by the following linear system

$$\sum_{j=1}^{q_1} w_{n,j}^{(1)} (t_j)^{\sigma_r} = \frac{1}{\Gamma(\alpha)} \int_{t_n - \tau}^{t_n} (t_n - s)^{\alpha-1} s^{\sigma_r} ds - \sum_{k=0}^2 \phi_k^{(2)} (t_{n-k})^{\sigma_r}, \quad 1 \leq r \leq q_1, \quad (4.2)$$

where  $\{\phi_k^{(2)}\}$  are given by (3.16).

For the approximation of the history part (3.8), the error mainly comes from solving ODE (3.10) with non-smooth input  $u(s)$ , which is the solution of the considered FDE. Next, we introduce how to approximate the history part with high

accuracy. What we need to do is introduce suitable correction terms for calculating  $e^{-\lambda_j^{(\ell)}\tau} \int_{t_n}^{t_{n+1}} e^{\lambda_j^{(\ell)}(s-t_n)} I_\tau^{(p,n)} u(s) ds$  in (3.12), which is given by

$$e^{-\lambda_j^{(\ell)}\tau} \int_{t_n}^{t_{n+1}} e^{\lambda_j^{(\ell)}(s-t_n)} I_\tau^{(p,n)} u(s) ds = \sum_{k=0}^p \psi_k^{(p)} u(t_{n-k}) + \sum_{j=1}^{q_2} w_{n,j}^{(2)} (u_j - u_0), \quad (4.3)$$

where the starting weights  $\{w_{n,j}^{(2)}\}$  are chosen such that

$$e^{-\lambda_j^{(\ell)}\tau} \int_{t_n}^{t_{n+1}} e^{\lambda_j^{(\ell)}(s-t_n)} u(s) ds = \sum_{k=0}^p \psi_k^{(p)} u(t_{n-k}) + \sum_{j=1}^{q_2} w_{n,j}^{(2)} (u_j - u_0) \quad (4.4)$$

for  $u(t) = t^{\sigma_k}$  ( $k = 1, 2, \dots, q_2$ ). For quadratic interpolation, the starting weights  $\{w_{n,j}^{(2)}\}$  can be derived by solving the following linear system

$$\sum_{j=1}^{q_2} w_{n,j}^{(2)} (t_j)^{\sigma_r} = e^{-\lambda_j^{(\ell)}\tau} \int_{t_n}^{t_{n+1}} e^{\lambda_j^{(\ell)}(s-t_n)} s^{\sigma_r} ds - \sum_{k=0}^2 \psi_k^{(2)} (t_{n-k})^{\sigma_r}, \quad 1 \leq r \leq q_2, \quad (4.5)$$

where  $\{\psi_k^{(2)}\}$  are given by (3.14). Therefore, Eq. (3.13) becomes

$$y_{n+1} = e^{-\lambda_j^{(\ell)}\tau} y_n + \psi_2^{(2)} u_{n-2} + \psi_1^{(2)} u_{n-1} + \psi_0^{(2)} u_n + \sum_{j=1}^{q_2} w_{n,j}^{(2)} (u_j - u_0). \quad (4.6)$$

Now, we obtain our fast convolution with correction terms, which is similar to that in the previous section, where we just need to replace (3.13) and (3.15) with (4.6) and (4.1), respectively.

**5. Short memory principle with lag terms.** In this section, we generalize the fast convolution in the previous section to resolve the short memory principle (see [5, 26]). Here we will keep the history part and approximate it with high accuracy and low computational cost.

Let  $\Delta T$  be a positive constant. For  $t > \Delta T$ , we divide the convolution  $\int_0^t k_\alpha(t-s)u(s) ds$  into the following two parts

$$\begin{aligned} \oint_0^t k_\alpha(t-s)u(s) ds &= \oint_{t-\Delta T}^t k_\alpha(t-s)u(s) ds + \int_0^{t-\Delta T} k_\alpha(t-s)u(s) ds \\ &\equiv L_{\Delta T}^\alpha(u, t) + H_{\Delta T}^\alpha(u, t). \end{aligned} \quad (5.1)$$

Here we still call  $L_{\Delta T}^\alpha(u, t)$  and  $H_{\Delta T}^\alpha(u, t)$  the local and history parts, respectively. If we drop the history part in (5.1), then the remaining part  $L_{\Delta T}^\alpha(u, t)$  is the famous short memory principle rule (see [26]). However, the short memory principle has not been widely applied, since  $L_{\Delta T}^\alpha(u, t)$  is not a good approximation of  $\int_0^t k_\alpha(t-s)u(s) ds$ . Our goal is to develop a good numerical approximation of  $H_{\Delta T}^\alpha(u, t)$ , such that the storage and computational cost are comparable with that of the numerical methods for the local part  $L_{\Delta T}^\alpha(u, t)$ . In fact,  $L_{\Delta T}^\alpha(u, t)$  is just the fractional operator defined on the interval  $[t - \Delta T, t]$ , thus the known methods can be applied, see [2, 5, 9, 11, 19, 21, 29, 38, 39].

Next, we are focused on the discretization of  $H_{\Delta T}^\alpha(u, t)$ . We can still make use of the original structure of the fast convolution in Section 4, which is illustrated below.

- Step A) Decompose  $\int_0^t k_\alpha(t-s)u(s)ds$  into two parts as shown by (5.1).
- Step B) Assume that  $\Delta T = n_0\tau = t_{n_0}$ . For every  $t = t_n, n \geq n_0$ , let  $L$  be the smallest integer satisfying  $t_{n-n_0+1} < 2B^L\tau$ . For  $\ell = 1, 2, \dots, L-1$ , determine the integer  $q_\ell$  such that

$$s_\ell = q_\ell B^\ell \tau \quad \text{satisfies} \quad t_{n-n_0+1} - s_\ell \in [B^\ell \tau, (2B^\ell - 1)\tau]. \quad (5.2)$$

Set  $s_0 = t_{n-n_0+1} - \tau$  and  $s_L = 0$ .

- Step C) Let  $\hat{t}_n = t_n - \Delta T + \tau$ , then the history part  $H_{\Delta T}^\alpha(u, t)$  is discretized by

$$\begin{aligned} H_{\Delta T}^\alpha(u, t_n) &= \frac{\sin(\alpha\pi)}{\pi} \int_0^{\hat{t}_n - \tau} \int_0^\infty \lambda^{-\alpha} e^{-(\Delta T - \tau)} e^{-(\hat{t}_n - s)\lambda} u(s) d\lambda ds \\ &= \frac{\sin(\alpha\pi)}{\pi} \sum_{\ell=1}^L \int_0^\infty \lambda^{-\alpha} e^{-(T_{\ell-1} + \Delta T - \tau)\lambda} e^{-(\hat{t}_n - s_{\ell-1} - T_{\ell-1})\lambda} y(s_{\ell-1}, s_\ell, \lambda) d\lambda \quad (5.3) \\ &\approx \frac{\sin(\alpha\pi)}{\pi} \sum_{\ell=1}^L \sum_{j=0}^{\kappa(N)} \omega_j^{(\ell)} e^{-(\hat{t}_n - s_{\ell-1} - T_{\ell-1})\lambda_j^{(\ell)}} y(s_{\ell-1}, s_\ell, \lambda_j^{(\ell)}) = H_{T, \tau}^{(\alpha, n, q_2)} u, \end{aligned}$$

where  $\{\omega_j^{(\ell)}\}$  and  $\{\lambda_j^{(\ell)}\}$  are the Gauss–Laguerre quadrature weights and points that correspond to the weight function  $\lambda^{-\alpha} e^{-(T_{\ell-1} + \Delta T - \tau)\lambda}$ . Note that  $y(s_{\ell-1}, s_\ell, \lambda_j^{(\ell)})$  in (5.3) is obtained by solving ODE (3.10) with  $q_2$  correction terms, i.e.  $y(s_{\ell-1}, s_\ell, \lambda_j^{(\ell)})$  is resolved by (4.6).  $\kappa(N)$  is the number of quadrature points used in the truncated Gauss–Laguerre quadrature, see (6.5).

- Step D) Approximate the local part  $L_{\Delta T}^\alpha(u, t)$  by (5.7) or (5.8).

Next, we consider the approximation of the local part. The local part  $L_{\Delta T}^\alpha(u, t)$  is equivalent to the following integral

$$L_{\Delta T}^\alpha(u, t) = \frac{1}{\Gamma(\alpha)} \int_0^{\Delta T} (\Delta T - s)^{\alpha-1} u(s + t - \Delta T) ds,$$

which can be discretized by using known time stepping methods, such as interpolation methods [7, 9, 29] and fractional linear multi-step methods [11, 19, 38, 39]. In this work, we apply quadratic interpolation and we need only to consider the approximation of  $\frac{1}{\Gamma(\alpha)} \int_0^t (t-s)^{\alpha-1} u(s) ds$ . Define the global piecewise interpolation  $I_\tau^{(p)}$  as follows

$$I_\tau^{(p)} u(t) = \begin{cases} I_\tau^{(p,p-1)} u(t), & t \in [t_{n-1}, t_n], n = 1, 2, \dots, p-1, \\ I_\tau^{(p,n)} u(t), & t \in [t_{n-1}, t_n], n \geq p, \end{cases} \quad (5.4)$$

where  $I_\tau^{(p,n)}$  is defined in (3.11). Replacing  $u(t)$  with  $I_\tau^{(2)} u(t)$ , we have

$$\begin{aligned} [D_{0,t}^{-\alpha} u(t)]_{t=t_n} &\approx [D_{0,t}^{-\alpha} I_\tau^{(2)} u(t)]_{t=t_n} = \frac{\tau^\alpha}{\Gamma(3+\alpha)} \left[ d_n^{(\alpha,0)} u_0 + d_n^{(\alpha,1)} u_1 + d_n^{(\alpha,2)} u_2 \right. \\ &\quad \left. + \sum_{k=1}^{n-1} (a_{n-k}^{(\alpha)} u_{k-1} + b_{n-k}^{(\alpha)} u_k + c_{n-k}^{(\alpha)} u_{k+1}) \right] + \tau^\alpha \sum_{k=1}^m \hat{w}_{n,k}^{(\alpha)} u_k = L_\tau^{(\alpha, n, m)} u, \end{aligned} \quad (5.5)$$

where  $a_n^{(\alpha)}, b_n^{(\alpha)}, c_n^{(\alpha)}$ , and  $d_n^{(\alpha,q)}$  ( $q = 0, 1, 2$ ) are defined by

$$\begin{aligned}
a_n^{(\alpha)} &= \ell_n^{(2+\alpha)} - (1 + \frac{\alpha}{2}) \left[ n^{1+\alpha} + (n-1)^{1+\alpha} \right], \\
b_n^{(\alpha)} &= - \left[ 2\ell_n^{(2+\alpha)} - 2(2+\alpha)(n-1)^{1+\alpha} - (1+\alpha)(2+\alpha)n^\alpha \right], \\
c_n^{(\alpha)} &= \ell_n^{(2+\alpha)} + (1 + \frac{\alpha}{2}) \left[ n^{1+\alpha} - 3(n-1)^{1+\alpha} \right] - (1+\alpha)(2+\alpha)(n-1)^\alpha, \\
d_n^{(\alpha,0)} &= \ell_n^{(2+\alpha)} - (1 + \frac{\alpha}{2}) \left[ 3n^{1+\alpha} - (n-1)^{1+\alpha} \right] + (1+\alpha)(2+\alpha)n^\alpha, \\
d_n^{(\alpha,1)} &= - \left[ 2\ell_n^{(2+\alpha)} - 2(2+\alpha)n^{1+\alpha} + (1+\alpha)(2+\alpha)(n-1)^\alpha \right], \\
d_n^{(\alpha,2)} &= \ell_n^{(2+\alpha)} - (1 + \frac{\alpha}{2}) \left[ n^{1+\alpha} + (n-1)^{1+\alpha} \right], \\
\ell_n^{(\alpha)} &= n^\alpha - (n-1)^\alpha.
\end{aligned} \tag{5.6}$$

The starting weights  $\{\hat{w}_{n,k}^{(\alpha)}\}$  are chosen such that (5.5) is exact, i.e.,  $[D_{0,t}^{-\alpha} u(t)]_{t=t_n} = L_{\tau}^{(\alpha,n,m)} u$ , for  $u(t) = t^{\sigma_r}$  ( $1 \leq r \leq m$ ),  $\sigma_r < \sigma_{r+1}$ . We refer readers to [2, 8, 19, 42] for more details on how to derive the starting weights and their related properties. Eq. (5.5) will be used to discretize the Caputo fractional derivative in the numerical simulations in the following section. From (5.5), we can derive the discretization of  $L_{\Delta T}^{\alpha}(u, t_n)$  as follows

$$\begin{aligned}
L_{\Delta T}^{\alpha}(u, t_n) &= \frac{1}{\Gamma(\alpha)} \int_0^{\Delta T} (\Delta T - s)^{\alpha-1} (u(s + t_{n-n_0}) - u_{n-n_0}) \, ds + \frac{\Delta T^\alpha}{\Gamma(1+\alpha)} u_{n-n_0} \\
&\approx \frac{\tau^\alpha}{\Gamma(3+\alpha)} \left[ d_{n_0}^{(\alpha,0)} \tilde{u}_{n-n_0}, d_{n_0}^{(\alpha,1)} \tilde{u}_{n-n_0+1} + d_{n_0}^{(\alpha,2)} \tilde{u}_{n-n_0+2} \right. \\
&\quad \left. + \sum_{k=1}^{n_0-1} \left( a_{n-k}^{(\alpha)} \tilde{u}_{n-n_0+k-1} + b_{n-k}^{(\alpha)} \tilde{u}_{n-n_0+k} + c_{n-k}^{(\alpha)} \tilde{u}_{n-n_0+k+1} \right) \right] \\
&\quad + \tau^\alpha \sum_{k=1}^m \hat{w}_{n,k}^{(\alpha)} \tilde{u}_{n-n_0+k} + \frac{\Delta T^\alpha}{\Gamma(1+\alpha)} u_{n-n_0} = L_{\Delta T, \tau}^{(\alpha,n,m)} u,
\end{aligned} \tag{5.7}$$

where  $n_0 = \Delta T / \tau$ ,  $\tilde{u}_{n-n_0+k} = u_{n-n_0+k} - u_{n-n_0}$ ,  $u_n = u(t_n)$ .

REMARK 1. The correction terms in (5.7) can be dropped due to the smoothness of  $u(t)$  when  $t \gg \Delta T$ , see [7, 9]. To this end, we can directly apply (5.5) to discretize  $L_T^{\alpha}(u, t)$  and obtain

$$\begin{aligned}
L_{\Delta T}^{\alpha}(u, t_n) \approx L_{\Delta T, \tau}^{(\alpha,n)} u &= \frac{\tau^\alpha}{\Gamma(3+\alpha)} \left[ d_{n_0}^{(\alpha,0)} u_{n-n_0} + d_{n_0}^{(\alpha,1)} u_{n-n_0+1} + d_{n_0}^{(\alpha,2)} u_{n-n_0+2} \right. \\
&\quad \left. + \sum_{k=1}^{n_0-1} \left( a_{n-k}^{(\alpha)} u_{n-n_0+k-1} + b_{n-k}^{(\alpha)} u_{n-n_0+k} + c_{n-k}^{(\alpha)} u_{n-n_0+k+1} \right) \right].
\end{aligned} \tag{5.8}$$

If  $\Delta T = \tau$ , then we let  $L_{\Delta T, \tau}^{(\alpha,n)} = L_{\tau}^{(\alpha,n,2)}$ , where  $L_{\tau}^{(\alpha,n,2)}$  is defined by (3.15). The fast method Steps A)-D) also reduces to the fast method in Section 3 for  $\Delta T = \tau$ .

Next, we analyze the complexity of the present fast method. For the local part, the memory requirement is  $O(n_0)$  and the computational cost of (5.7) or (5.8) is  $O(n_0(n_T - n_0))$  for all  $n_0 < n \leq n_T$ . For the history part, we have  $O(\kappa(N) \log(n_T - n_0))$  active memory and  $O(\kappa(N)(n_T - n_0) \log(n_T - n_0))$  operations. Hence, the overall active memory and computational cost are  $O(n_0 + \kappa(N) \log(n_T - n_0))$  and  $O(n_0(n_T - n_0) + \kappa(N) \log(n_T - n_0))$ , respectively.

**6. Determination of the basis  $B$ .** In Section 3, we show that the Gauss–Laguerre quadrature displays superior performance in the approximation of the kernel  $k_\alpha(t - s)$  used in the fractional operator. Here we will further study the Gauss–Laguerre quadrature rule, which provides a guideline to choose the suitable basis  $B$  such that high accuracy is kept and less storage is required.

In (3.8), we note that the integral of the following type

$$\int_0^\infty \lambda^{-\alpha} e^{-T\lambda} e^{-t\lambda} y(\lambda) d\lambda \quad (6.1)$$

is discretized by the Gauss–Laguerre quadrature. Theoretically,  $e^{-t\lambda} y(\lambda)$  used in this paper is an infinitely differentiable function, whose smoothness is independent of the solutions of the considered FDEs, hence spectral convergence should be achieved when the number of the quadrature points is sufficiently large for any  $t, T > 0$ , see [22]. Moreover,  $e^{-t\lambda} y(\lambda)$  is also an exponentially decreasing function and decays rapidly as  $t$  increases. Therefore, more quadrature points are needed near  $\lambda = 0$  to achieve the desired accuracy when  $t$  is sufficiently large, which may be not practical due to the large roundoff errors with double precision computation. Our aim below is to use a suitable number of quadrature points and find a suitable  $B$  in order that high accuracy is obtained and less memory is used.

For a given  $T$  in (6.1), our concern is how to determine a sufficiently large  $t = t_{\max}$  in order that high accuracy up to  $\epsilon$  is kept for all  $t \in [0, t_{\max}]$ . Obviously,  $t_{\max}$  depends on the number of quadrature points and  $T$ . To this end, we need only to study the error of the following quadrature

$$\int_0^\infty \hat{\lambda}^{-\alpha} e^{-\hat{\lambda}} e^{-t\hat{\lambda}} d\hat{\lambda} \approx \sum_{j=0}^N \hat{w}_j e^{-t\hat{\lambda}_j}, \quad t \geq 0, \alpha < 1, \quad (6.2)$$

where  $\{\hat{\lambda}_j\}$  and  $\{\hat{w}_j\}$  are, respectively, the Gauss–Laguerre quadrature points and weights that correspond to the weight function  $\hat{\lambda}^{-\alpha} e^{-\hat{\lambda}}$ . Let  $\hat{\lambda} = T\lambda$ ,  $\hat{\lambda}_j = T\lambda_j$ , and  $w_j = T^{\alpha-1} \hat{w}_j$ . Then we have from (6.1) and (6.2)

$$\begin{aligned} \int_0^\infty \lambda^{-\alpha} e^{-T\lambda} e^{-t\lambda} y(\lambda) d\lambda &= T^{\alpha-1} \int_0^\infty \hat{\lambda}^{-\alpha} e^{-\hat{\lambda}} e^{-\frac{t}{T}\hat{\lambda}} y(T^{-1}\hat{\lambda}) d\hat{\lambda} \\ &\approx T^{\alpha-1} \sum_{j=0}^N \hat{w}_j e^{-\frac{t}{T}\hat{\lambda}_j} y(T^{-1}\hat{\lambda}_j) \\ &= \sum_{j=0}^N w_j e^{-t\lambda_j} y(\lambda_j). \end{aligned} \quad (6.3)$$

The two formulas (6.2) and (6.3) have almost similar relative discretization errors, which will be verified in the following, see (6.6).

Thanks to the fast decreasing quadrature weights of the Gauss–Laguerre quadrature,  $\{\hat{w}_j, j = j_0, j_0 + 1, \dots, N\}$  is a fast decreasing sequence when  $j > j_0$ ,  $j_0$  is a nonnegative integer. The truncated Gauss–Laguerre quadrature  $\int_0^\infty \hat{\lambda}^{-\alpha} e^{-\hat{\lambda}} e^{-t\hat{\lambda}} d\hat{\lambda} \approx \sum_{0 < \hat{\lambda}_j < 4\theta N} \hat{w}_j e^{-t\hat{\lambda}_j}$  with the same accuracy as (6.2) was developed in [22], where  $0 < \theta < 1$  is arbitrarily chosen. For simplicity, we will use the following truncated

quadrature rule

$$\int_0^\infty \lambda^{-\alpha} e^{-T\lambda} e^{-t\lambda} y(\lambda) d\lambda \approx \sum_{j=0}^{\kappa(N)} w_j e^{-t\lambda_j} y(\lambda_j), \quad (6.4)$$

where  $\kappa(N)$  is uniquely determined by

$$\kappa(N) = j, \quad \hat{w}_{j+1} < \epsilon_0 \leq \hat{w}_j, \quad j = j_0, j_0 + 1, \dots, N \quad (6.5)$$

for a given  $\epsilon_0$ . We choose  $\epsilon_0 = 10^{-16}$  for the numerical simulations reported in this paper, which is close to machine precision. Numerical simulations show that the truncated quadrature (6.4) satisfies accuracy requirement. We find that  $\kappa(N)$  is far less than  $N$ , so that storage and computational costs decrease significantly, see  $\kappa(N)$  in Table 6.3. We always use (6.4) in numerical simulations.

The discretization error of (6.4) depends on the ratio  $t/T$  to some extent if  $y(t)$  is smooth and bounded, which is verified in the following example.

EXAMPLE 6.1. *Check the accuracy of (6.4) with  $y(\lambda) = e^{-\sigma\lambda}$ ,  $\operatorname{Re}(\sigma) \geq 0$ . It is easy to obtain  $\int_0^\infty \lambda^{-\alpha} e^{-T\lambda} e^{-t\lambda} y(\lambda) d\lambda = (T + t + \sigma)^{\alpha-1} \Gamma(1 - \alpha)$ . Thus, the relative pointwise error of (6.4) is defined as*

$$e(T, t, \sigma) = \frac{|(1 + (t + \sigma)/T)^{\alpha-1} \Gamma(1 - \alpha) - \sum_{j=0}^{\kappa(N)} \hat{w}_j e^{-\frac{t}{T}\hat{\lambda}_j} y(T^{-1}\hat{\lambda}_j)|}{|(1 + (t + \sigma)/T)^{\alpha-1} \Gamma(1 - \alpha)|}. \quad (6.6)$$

For simplicity, we first let  $T = 1$  and see how  $t$  influences the accuracy of the quadrature (6.4); the relative error  $e(1, t, \sigma)$  of (6.4) is shown in Figure 6.1(a) for  $-\alpha = 0.9$  and  $\sigma = i$ . We observe two important features from Figure 6.1(a):

- (i) For a fixed  $N$ , there exists a  $t_{\max}$  such that certain accuracy is kept for all  $t \in [0, t_{\max}]$ . For example, for  $N = 1024$  and  $\alpha = -0.9$ , an accuracy up to  $10^{-13}$  was achieved for all  $t \in [0, t_{\max}]$ ,  $t_{\max} \approx 120$ . For other choices of  $\alpha < 1$ , similar behavior is also observed, which is not presented here.
- (ii) For a fixed  $\epsilon$ , we observe that  $t_{\max} = t_{\max}(\epsilon, N)$  increases as  $N$  increases, and  $\frac{t_{\max}(\epsilon, 2N)}{t_{\max}(\epsilon, N)} \approx 2 = \frac{2N}{N}$  for the accuracy level  $\epsilon = 10^{-13}$ , see Figure 6.1(a). This observation encourages us to use a moderately large  $N$  in order that less storage will be used in real applications, hence the computational cost will be reduced. For the accuracy level  $\epsilon = 10^{-10}$ , we have the following more generalized observation

$$\frac{t_{\max}(\epsilon, N_2)}{t_{\max}(\epsilon, N_1)} \approx \frac{N_2}{N_1}, \quad N_1, N_2 < 10^4, \alpha \in (-1, 1). \quad (6.7)$$

Figure 6.1(b) shows similar results as those in Figure 6.1(a), while we apply the Gauss–Laguerre quadrature with up to  $2^{13} = 8192$  quadrature points, and obtain  $t_{\max}(\epsilon, 2^{13}) \approx 1250$  for  $\epsilon = 10^{-10}$  and  $\alpha = -0.2$ . Tables 6.1 and 6.2 show  $t_{\max}(\epsilon, N)$  and the ratio  $t_{\max}(\epsilon, N_k)/t_{\max}(\epsilon, N_{k-1})$  for  $\alpha = 0.8$  and  $\alpha = -0.5$ , respectively, which agrees well with the observation (6.7).

Table 6.3 shows the values of the important parameter  $\kappa(N)$ . We find that  $\kappa(N)$  is far less than  $N$  as  $N$  increases. For example,  $\kappa(2^{13}) = \kappa(8192) = 356 \ll 8192$  for  $\alpha = -0.8$ , which means the storage and computation cost will be reduced greatly when the truncated quadrature rule (6.4) is applied. Further calculation and experiments reveal that  $\frac{\kappa(2N)}{\kappa(N)} \approx 1.4$  for  $\alpha \in (-1, 1)$ , see numerical results in Table 6.3.

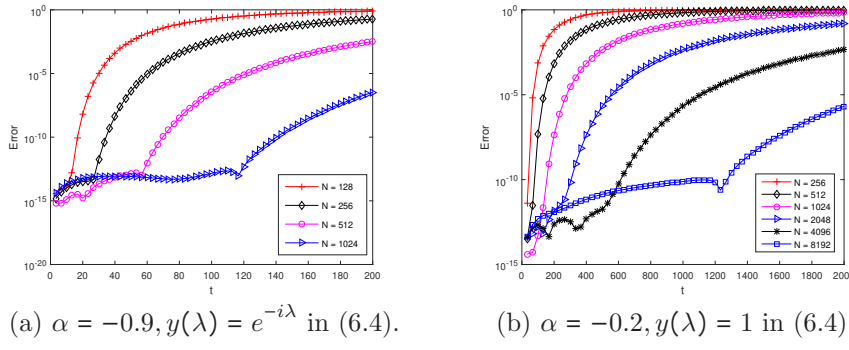


FIG. 6.1. The relative error of the Gauss-Laguerre quadrature (6.4) with respect to the weight function  $\omega = \lambda^{-\alpha} e^{-\lambda}$ .

TABLE 6.1  
 $N_k = 2^{k+7}, \alpha = 0.8, T = 1, \epsilon = p \times 10^{-10}, y(t) = 1, t_{\max}(N) = t_{\max}(\epsilon, N)$ .

	$p$	$k = 1$	$k = 2$	$k = 3$	$k = 4$	$k = 5$	$k = 6$
$t_{\max}(N_k)$	1	45.89	92.760	186.47	373.99	748.28	1488.06
$t_{\max}(N_k)/t_{\max}(N_{k-1})$		-	2.0214	2.0102	2.0056	2.0008	1.9886
$t_{\max}(N_k)$	3	48.34	97.650	196.26	393.53	787.78	1572.63
$t_{\max}(N_k)/t_{\max}(N_{k-1})$		-	2.0201	2.0098	2.0051	2.0018	1.9963
$t_{\max}(N_k)$	5	49.56	100.10	201.16	403.33	807.47	1613.32
$t_{\max}(N_k)/t_{\max}(N_{k-1})$		-	2.0198	2.0096	2.0050	2.0020	1.9980
$t_{\max}(N_k)$	7	50.40	101.78	204.53	410.05	820.95	1640.91
$t_{\max}(N_k)/t_{\max}(N_{k-1})$		-	2.0194	2.0095	2.0048	2.0021	1.9988

TABLE 6.2  
 $N_k = 2^{k+7}, \alpha = -0.5, T = 1, \epsilon = p \times 10^{-10}, y(t) = 1, t_{\max}(N) = t_{\max}(\epsilon, N)$ .

	$p$	$k = 1$	$k = 2$	$k = 3$	$k = 4$	$k = 5$	$k = 6$
$t_{\max}(N_k)$	1	36.06	73.010	146.97	293.83	596.00	1183.86
$t_{\max}(N_k)/t_{\max}(N_{k-1})$		-	2.0247	2.0130	1.9993	2.0284	1.9863
$t_{\max}(N_k)$	3	37.65	76.190	153.28	307.03	617.94	1233.70
$t_{\max}(N_k)/t_{\max}(N_{k-1})$		-	2.0236	2.0118	2.0031	2.0126	1.9965
$t_{\max}(N_k)$	5	38.44	77.760	156.41	313.44	629.69	1258.57
$t_{\max}(N_k)/t_{\max}(N_{k-1})$		-	2.0229	2.0114	2.0040	2.0090	1.9987
$t_{\max}(N_k)$	7	38.98	78.830	158.55	317.78	637.89	1275.57
$t_{\max}(N_k)/t_{\max}(N_{k-1})$		-	2.0223	2.0113	2.0043	2.0073	1.9997

TABLE 6.3

The number of the truncated quadrature points  $\kappa(N_k)$  that corresponds to the weight function  $\omega(\lambda) = \lambda^{-\alpha} e^{-\lambda}, N_k = 2^{k+7}$ .

	$\alpha$	$k = 1$	$k = 2$	$k = 3$	$k = 4$	$k = 5$	$k = 6$
$\kappa(N_k)$	-0.8	63	90	127	179	252	356
$\kappa(N_k)/\kappa(N_{k-1})$	-0.8	-	1.4286	1.4111	1.4094	1.4078	1.4127
$\kappa(N_k)$	-0.2	62	88	124	174	245	345
$\kappa(N_k)/\kappa(N_{k-1})$	-0.2	-	1.4194	1.4091	1.4032	1.4080	1.4082
$\kappa(N_k)$	0.2	61	86	121	171	240	338
$\kappa(N_k)/\kappa(N_{k-1})$	0.2	-	1.4098	1.4070	1.4132	1.4035	1.4083
$\kappa(N_k)$	0.8	59	84	118	166	233	328
$\kappa(N_k)/\kappa(N_{k-1})$	0.8	-	1.4237	1.4048	1.4068	1.4036	1.4077

Figure 6.2 shows that the relative error  $e(T, t, \sigma)$  of (6.4) mainly depends on the

ratio  $t/T$  when  $t$  is sufficiently large for  $\alpha = 0.9, 0.2$ . For other cases of  $\alpha < 1$ , we have similar results, which are not shown here.

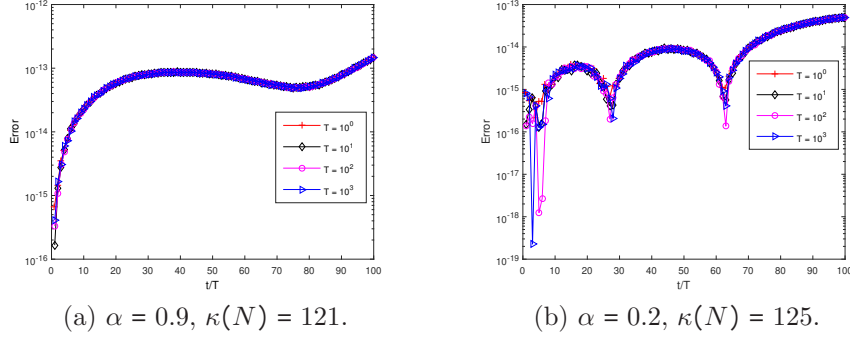


FIG. 6.2. The relative error of the Gauss-Laguerre quadrature with respect to the weight function  $\omega = \lambda^{-\alpha} e^{-T\lambda}$ ,  $y = e^{-(t+i)\lambda}$ ,  $N = 1024$ .

Next, we discuss how to determine the basis  $B$ , such that the desired accuracy can be reached. Theoretically, we can obtain spectral accuracy by choosing very large  $N$  in the Gauss-Laguerre quadrature (6.4). Given a positive integer  $N$ , the discretization error of (5.3) depends on the ratio  $\frac{\hat{t}_n - s_{\ell-1} - T_{\ell-1}}{T_{\ell-1} + T - \tau}$ . From the previous observation (see Figure 6.2), we should have  $\frac{\hat{t}_n - s_{\ell-1} - T_{\ell-1}}{T_{\ell-1} + T - \tau} \leq t_{\max}(\epsilon, N)$  if we want to obtain the accuracy up to the level of  $\epsilon$ . Since  $\hat{t}_n - s_{\ell-1} \in [B^{\ell-1}\tau, (2B^\ell - 1)\tau]$  and  $T_\ell = B^\ell\tau$ , we just need  $\frac{\hat{t}_n - s_{\ell-1} - T_{\ell-1}}{T_{\ell-1} + T - \tau} = \frac{(2B^\ell - 1)\tau - B^{\ell-1}\tau}{B^{\ell-1}\tau + T - \tau} \leq \frac{(2B^\ell - 1)\tau - B^{\ell-1}\tau}{B^{\ell-1}\tau} \leq t_{\max}(\epsilon, N)$ , which leads to  $B \leq (t_{\max}(\epsilon, N) + 1 + B^{1-\ell})/2 \rightarrow t_{\max}(\epsilon, N)/2 + 1/2$  as  $\ell \rightarrow \infty$ . Hence, we have the following criteria for choosing the basis

$$B \leq \frac{1}{2} (1 + t_{\max}(\epsilon, N)). \quad (6.8)$$

Here  $t_{\max}(\epsilon, N)$  can be obtained by choosing a suitable  $N$  such that  $e(t, 1, 0) \leq \epsilon$ , where  $e(t, 1, 0)$  is defined by (6.6). In real applications,  $B$  can be a slightly larger than  $\frac{1}{2}(1 + t_{\max}(\epsilon, N))$ .

We still consider Example 3.1, while we choose different  $B$  in the numerical simulations. The maximum relative errors  $\|e^{(2)}\|_\infty = \max_{0 < n \leq 1000/\tau} e^{(2)}(t_n)$  (see (3.20)) for  $\alpha = 0.8$  are shown in Table 6.4. In Table 6.4, we first choose  $B = B^* = \lceil \frac{1}{2}(1 + t_{\max}(\epsilon, N)) \rceil$  in the computation, then we increase  $B$  up to  $t_{\max}(\epsilon, N)$ . We find that as  $B$  increases, the accuracy decreases. If  $2 \leq B < B^*$ , then even higher accuracy is obtained, see Table 6.5. We also test the fast convolution in [20] for large basis  $B$ . It does not keep high accuracy using the Talbot contour as that in Figure 3.2, and the results are not provided here.

At last in this section, we investigate the storage requirement for calculating the history part  $H_{\Delta T}^\alpha(u, t_n)$  (see (5.3)) for  $t_n \in [\Delta T, 1183.86]$ ,  $\Delta T = 1$ , and  $\tau = 0.01$ . Here we fix a precision  $\epsilon = 10^{-10}$  to approximate the kernel  $k_\alpha(t)$ , hence  $t_{\max}(\epsilon, N)$  can be derived by letting  $e(1, t, 0) \leq \epsilon$  (see (6.6)). Then  $B = B^* = \lceil \frac{1}{2}(1 + t_{\max}(\epsilon, N)) \rceil$  is obtained, which is almost an optimal choice, since the discretization error from the kernel  $k_\alpha(t)$  increases as  $B$  increases (or does not increase) and  $B > B^*$  (or  $B \leq B^*$ ). We show the memory requirement in Table 6.6, in which  $L$  denotes the maximum

TABLE 6.4

The maximum relative errors  $\|e^{(2)}\|_\infty$  of the history part  $H_{\Delta T}^\alpha(u, t)$ ,  $u = 1 + t$ ,  $t \in [\Delta T, 1000]$ ,  $N_k = 2^{k+7}$ ,  $\epsilon = 10^{-10}$ ,  $\Delta T = \tau$ ,  $\alpha = 0.8$ .

	$k = 1$	$k = 2$	$k = 3$	$k = 4$	$k = 5$	$k = 6$
$t_{\max}(N_k)$	45.89	92.760	186.47	373.99	748.28	1488.06
$B^*$	24	47	94	188	375	745
$\ e^{(2)}\ _\infty$	3.2895e-12	2.0192e-12	2.0944e-12	1.9285e-12	2.3426e-12	1.9246e-12
$B$	30	60	120	240	480	960
$\ e^{(2)}\ _\infty$	3.1859e-10	3.0886e-10	3.0309e-10	2.8601e-10	2.9028e-10	2.9360e-10
$B$	35	70	140	280	560	1120
$\ e^{(2)}\ _\infty$	4.5930e-09	4.2659e-09	4.1879e-09	3.9936e-09	4.0292e-09	4.0472e-09
$B$	40	80	160	320	640	1280
$\ e^{(2)}\ _\infty$	3.4193e-08	3.1192e-08	2.9010e-08	2.9436e-08	2.9624e-08	2.9707e-08

TABLE 6.5

The maximum relative errors  $\|e^{(2)}\|_\infty$  of the history part  $H_{\Delta T}^\alpha(u, t)$ ,  $u = 1 + t$ ,  $t \in [\Delta T, 1000]$ ,  $N_k = 2^{k+7}$ ,  $\epsilon = 10^{-10}$ ,  $\Delta T = \tau$ ,  $\alpha = 0.8$ .

	$k = 1$	$k = 2$	$k = 3$	$k = 4$	$k = 5$	$k = 6$
$B$	14	27	54	108	215	425
$\ e^{(2)}\ _\infty$	4.3514e-13	2.7840e-13	4.1641e-13	2.5958e-13	2.6533e-13	9.0752e-13
$B$	10	10	10	10	10	10
$\ e^{(2)}\ _\infty$	3.9407e-13	3.6168e-13	1.8653e-13	1.5947e-13	6.0563e-14	4.0440e-14
$B$	4	7	14	28	55	105
$\ e^{(2)}\ _\infty$	3.7736e-13	1.7355e-13	4.2891e-13	2.8391e-13	6.4739e-13	1.5174e-13
$B$	2	2	2	2	2	2
$\ e^{(2)}\ _\infty$	1.4521e-13	4.5519e-14	1.7378e-13	5.0395e-14	9.1525e-14	5.3930e-14

number of subintervals  $I_\ell = [B^{\ell-1}\tau, (2B^\ell - 1)\tau]$  satisfying  $\forall t_n \in [\Delta T, 1183.86] = \bigcup_{1 \leq \ell \leq L} I_\ell$ , see (5.2). We can see that increasing the number of quadrature points does not always decrease the memory requirement. For a fixed  $N$  and a precision  $\epsilon$ , the optimal choice of the basis may be  $B = B^*$ , thus a suitably smaller  $N$  may be economical in real applications. It seems that we require much more memory for  $N = 2^{13}$ , see the last column in Table 6.6. In fact, we have  $e(1, t, 0) \leq 10^{-10}$  for  $N = 2^{13}$  and  $\forall t \in [1, 1183.86]$ , which implies we can choose any basis  $B$  satisfying  $(2B - 1)\tau \geq 1183.86$ , i.e.,  $B \geq 59194$ , such that an accuracy up to  $10^{-10}$  can be preserved for  $\forall t \in [1, 1183.86]$ , and the storage requirement is 350 instead of 1050. A suitably large  $N$  implies that we do not need to divide the whole interval  $[\Delta T, t_{\text{final}}]$  into exponentially growing intervals  $I_\ell$  as done in [1, 16, 14], where  $t_{\text{final}}$  in this work is a final time for solving a considered FDE.

TABLE 6.6

Memory requirement for computing the history part  $H_{\Delta T}^\alpha(u, t_n)$ ,  $\alpha = -0.5$ ,  $t_n \in [\Delta T, 1183.86]$ ,  $\Delta T = 1$ ,  $\tau = 0.01$ ,  $N_k = 2^{k+5}$ .

	$k = 0$	$k = 1$	$k = 2$	$k = 3$	$k = 4$	$k = 5$	$k = 6$	$k = 7$	$k = 8$
$t_{\max}(N_k)$	3.79	8.38	17.60	36.06	73.01	146.97	293.83	596.00	<b>1183.86</b>
$B$	3	5	10	19	38	74	148	299	<b>593</b>
$\kappa(N_k)$	21	31	44	63	89	125	177	249	<b>350</b>
$L$	13	9	6	5	4	4	3	3	<b>3</b>
$L\kappa(N_k)$	273	279	264	315	356	500	531	747	<b>1050</b>

**7. Numerical examples and applications.** In this section, three examples are presented to verify the effectiveness of the present fast method when it is applied to solve FDEs. All the algorithms are implemented using MATLAB 2016a, which were run in a 3.40 GHz PC having 16GB RAM and Windows 7 operating system.

EXAMPLE 7.1. Consider the following scalar FODE

$${}_C D_{0,t}^\alpha u(t) = -Au(t) + F(u, t), \quad u(0) = u_0, \quad t \in (0, T], \quad (7.1)$$

where  $0 < \alpha \leq 1$  and  $A \geq 0$ .

We present our fast numerical method for (7.1) as follows:

- Step i) For a given length  $\Delta T$ , find a suitable  $\tilde{T} > \Delta T$  such that  $\tilde{T} - \Delta T$  is far from the origin. For  $0 < n \leq \tilde{T}/\tau$ , find  $U_n$  such that

$$L_\tau^{(-\alpha,n,m)}(U - U_0) = -AU_n + F(U_n, t_n), \quad (7.2)$$

where  $L_\tau^{(-\alpha,n,m)}$  is defined in (5.5). One can easily see that the discretization  $L_\tau^{(-\alpha,n,m)}(U - U_0)$  is an approximation of  ${}_C D_{0,t}^\alpha u(t)$  at  $t = t_n$ , the convergence rate is  $(3 - \alpha)$  when  $u(t)$  is smooth. If  $\alpha = 1$ , then the discrete operator  $L_\tau^{(-\alpha,n,m)}$  is reduced to the classical second-order backward difference formula for the first-order derivative. See also related works [6, 12, 15, 17, 21, 37, 40].

- Step ii) For  $n > \tilde{T}/\tau$ , find  $U_n$  such that

$$L_{\Delta T, \tau}^{(-\alpha,n)}(U - U_0) + H_{\Delta T, \tau}^{(-\alpha,n,m)}(U - U_0) = -AU_n + F(U_n, t_n), \quad (7.3)$$

where  $H_{\Delta T, \tau}^{(-\alpha,n,m)}$  is defined by (5.3) and  $L_{\Delta T, \tau}^{(-\alpha,n)}$  is defined by (5.8). Eq. (7.3) is derived by applying the relation  ${}_C D_{0,t}^\alpha u(t) = {}_{RL} D_{0,t}^\alpha(u(t) - u(0))$ , the property (2.6), and Eq. (5.1), that is,

$$L_{\Delta T}^{-\alpha}(u - u(0), t) + H_{\Delta T}^{-\alpha}(u - u(0), t) = D_{0,t}^{(-\alpha)}(u(t) - u(0)) = {}_C D_{0,t}^\alpha u(t). \quad (7.4)$$

REMARK 2. We choose a suitable  $\tilde{T} > \Delta T$  such that no correction terms are needed to approximate  $L_{\Delta T}^{-\alpha}(u - u(0), t)$  in (7.4), which makes (7.3) much simpler.

The Newton method is used to solve the nonlinear system (7.2) and (7.3). The following two cases are considered in this example.

Case I: For the linear case of  $F = 0$ , the exact solution of (7.1) is

$$u(t) = E_\alpha(-At^\alpha),$$

where  $E_\alpha(t)$  is the Mittag-Leffler function defined by  $E_\alpha(t) = \sum_{k=0}^{\infty} \frac{t^k}{\Gamma(k\alpha+1)}$ .

Case II: Let  $F = u(1 - u^2)$  and the initial condition is taken as  $u_0 = 1$ .

The maximum error is defined by

$$\|e\|_\infty = \max_{0 \leq n \leq T/\tau} |e_n|, \quad e_n = u(t_n) - U_n, T = 40.$$

We always choose the memory length  $\Delta T = 0.5$ ,  $\tilde{T} = 1$ , the basis  $B = 5$ , the number of truncated quadrature points  $\kappa(N)$  in (5.3) is calculated by letting  $N = 64$ , and  $A = 1$  in this example. We will reset these parameters if needed.

The purpose of Case I is to check the effectiveness of the present fast method for non-smooth solutions. We demonstrate that adding correction terms improves the

accuracy of numerical solutions significantly. We first let  $\alpha = 0.8$ , the maximum error and the error at  $t = 40$  are shown in Tables 7.1 and 7.2, respectively. We can see that the expected convergence rate  $3 - \alpha$  is almost achieved by adding two or three correction terms, and the numerical solution at the final time is much more accurate than that near the origin. This phenomenon can be observed from the existing time-stepping methods for time-fractional differential equations, see [38, 39].

As the fractional order decreases, the singularity of the analytical solution becomes stronger. Tables 7.3 and 7.4, respectively, show the maximum errors and the errors at  $t = 40$  for  $\alpha = 0.1$ . We observe that the maximum error, which occurs near the origin, almost does not improve, though the step size decreases. We find that as the number of correction terms increases, the accuracy of the numerical solutions increases significantly. We need almost 31 correction terms to derive the expected global convergence rate  $3 - \alpha$  for  $\alpha = 0.1$ , which is impossible to achieve by double precision. The fact is a fewer number of correction terms is enough to yield satisfactory numerical solutions, which makes the present method more practical. We refer readers to [2, 3, 42] for more explanations and numerical results associated with this phenomenon.

TABLE 7.1

*The maximum error  $\|e\|_\infty$  of the method (7.2)–(7.3), Case I,  $\sigma_k = k\alpha$ ,  $\alpha = 0.8$ ,  $T = 40$ ,  $B = 5$ ,  $N = 64$ .*

$\tau$	$m = 0$	Order	$m = 1$	Order	$m = 2$	Order	$m = 3$	Order
$2^{-5}$	7.7443e-4		1.7260e-4		3.4374e-5		3.1589e-5	
$2^{-6}$	3.0512e-4	1.3438	5.9903e-5	1.5267	8.8273e-6	1.9613	7.5825e-6	2.0587
$2^{-7}$	2.0537e-4	0.5712	2.0299e-5	1.5612	2.1543e-6	2.0347	1.7383e-6	2.1250
$2^{-8}$	1.2807e-4	0.6813	6.8014e-6	1.5775	5.0794e-7	2.0845	3.8929e-7	2.1587
$2^{-9}$	7.6736e-5	0.7389	2.2642e-6	1.5868	1.1695e-7	2.1188	8.6092e-8	2.1769

TABLE 7.2

*The absolute error  $|e_n|$  ( $n = T/\tau$ ,  $T = 40$ ) of the method (7.2)–(7.3) at  $t = 40$ , Case I,  $\sigma_k = k\alpha$ ,  $\alpha = 0.8$ ,  $B = 5$ ,  $N = 64$ .*

$\tau$	$m = 0$	Order	$m = 1$	Order	$m = 2$	Order	$m = 3$	Order
$2^{-5}$	1.0421e-7		7.0537e-8		2.1916e-8		2.7419e-9	
$2^{-6}$	7.0735e-8	0.5590	2.0903e-8	1.7546	5.0083e-9	2.1296	1.0977e-9	1.3207
$2^{-7}$	3.9468e-8	0.8417	6.0963e-9	1.7777	1.1332e-9	2.1439	3.0136e-10	1.8649
$2^{-8}$	2.0607e-8	0.9376	1.7617e-9	1.7909	2.5405e-10	2.1572	7.3279e-11	2.0400
$2^{-9}$	1.0480e-8	0.9755	5.0677e-10	1.7976	5.6648e-11	2.1650	1.6772e-11	2.1274

TABLE 7.3

*The maximum error  $\|e\|_\infty$  of the method (7.2)–(7.3), Case I,  $\sigma_k = k\alpha$ ,  $\alpha = 0.1$ ,  $T = 40$ ,  $B = 5$ ,  $N = 64$ .*

$\tau$	$m = 0$	Order	$m = 1$	Order	$m = 3$	Order	$m = 5$	Order
$2^{-5}$	1.6112e-3		2.1034e-4		1.6342e-5		1.6333e-5	
$2^{-6}$	1.5674e-3	0.0397	1.9785e-4	0.0883	7.2707e-6	1.1684	7.2687e-6	1.1680
$2^{-7}$	1.5276e-3	0.0371	1.8577e-4	0.0909	3.2191e-6	1.1754	3.2187e-6	1.1752
$2^{-8}$	1.4887e-3	0.0372	1.7397e-4	0.0947	1.4920e-6	1.1094	1.4178e-6	1.1829
$2^{-9}$	1.4493e-3	0.0387	1.6245e-4	0.0989	1.2305e-6	0.2780	6.2126e-7	1.1904

Figure 7.1(a) shows the pointwise errors for a different memory length  $\Delta T = 0.1$ , where we choose the basis  $B = B^*$ ,  $B^* = \lceil \frac{T}{2\tau} + 1 \rceil$ ,  $\tau = 0.01$ ,  $T = 40$ . Such a choice

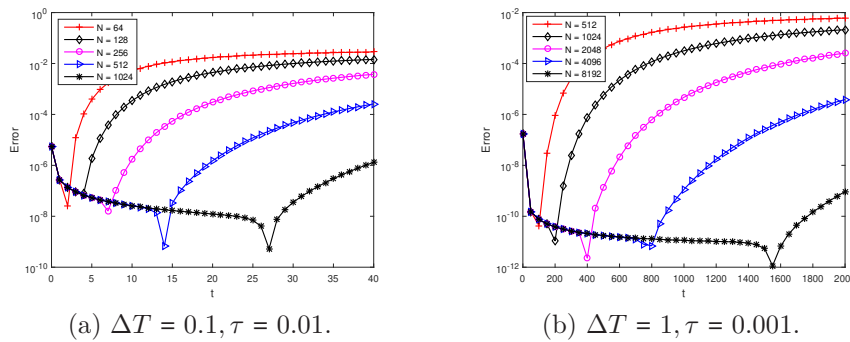
TABLE 7.4

The absolute error  $|e_n|$  ( $n = T/\tau, T = 40$ ) of the method (7.2)–(7.3) at  $t = 40$ , Case I,  $\sigma_k = k\alpha$ ,  $\alpha = 0.1$ ,  $B = 5$ ,  $N = 64$ .

$\tau$	$m = 0$	Order	$m = 1$	Order	$m = 3$	Order	$m = 5$	Order
$2^{-5}$	5.0428e-6		5.0727e-7		9.3366e-9		3.2336e-9	
$2^{-6}$	2.4984e-6	1.0132	2.4190e-7	1.0683	3.6666e-9	1.3485	7.8596e-10	2.0406
$2^{-7}$	1.2395e-6	1.0112	1.1530e-7	1.0691	1.5043e-9	1.2853	1.9479e-10	2.0125
$2^{-8}$	6.1543e-7	1.0101	5.4911e-8	1.0702	6.3341e-10	1.2479	4.9758e-11	1.9689
$2^{-9}$	3.0570e-7	1.0095	2.6128e-8	1.0715	2.6964e-10	1.2321	1.2519e-11	1.9909

of  $B$  insures that  $L$  in (5.3) is always one. We can choose any  $B > B^*$ , which does not affect the results; see also [14, 16] for similar approaches, where Gauss–Legendre quadrature was applied. We observe that for a fixed memory length  $\Delta T$  and  $N$ , numerical solutions keep a high accuracy level  $\epsilon$  for  $t \in [0, t_{\max}]$ , where  $t_{\max}$  depends on  $N, \Delta T, \epsilon$  and  $\alpha$ . For example for  $\epsilon = 10^{-8}$  and  $N = 1024$ ,  $t_{\max} \approx 28$  for  $\Delta T = 0.1$ . When  $t > t_{\max}$ , the accuracy decreases rapidly as  $t$  increases. If we increase  $N$  or/and  $\Delta T$ , then  $t_{\max}$  increases, which is beneficial for long time computation. This can be explained from Figure 6.2, see also related results shown in Tables 6.1 and 6.2. Figure 7.1(b) shows similar behavior as that of Figure 7.1(a), the difference is the smaller time stepsize  $\tau = 0.001$  is taken and a bigger  $N$  up to  $N = 8192$  is applied,  $B = \lceil \frac{T}{2\tau} + 1 \rceil$ ,  $T = 2000$ , and  $\Delta T = 1$ . The actual number of quadrature points used in the computation is  $\kappa(8192) = 345$  instead of 8192. We observe that very high accuracy up to  $10^{-10}$  is kept at  $t \approx 1800$  for  $\Delta T = 1$ , see Figure 7.1(b).

Next, we implement the present fast method for a longer time computation and compare it (solve (7.2)–(7.3)) with the direct convolution method (solve (7.2) for all  $n > 0$ ). We show in Figure 7.2(a) numerical solutions for  $t \in [0, T], T = 10000$ , where we choose  $\alpha = 0.1, 0.5, 0.9$ , and the time stepsize  $\tau = 0.01$ . In Figure 7.2(b), we plot the computational time of the two different convolutions with two correction terms applied. It shows that the computational cost of the fast convolution almost shows linear complexity with about  $O((\tilde{T}/\tau)^2 + \kappa(N)(T/\tau) \log(T/\tau))$  operations, which is much less than that of the direct convolution with  $O((T/\tau)^2)$  operations.

FIG. 7.1. Pointwise errors for Case I,  $m = 3, \sigma_k = k\alpha, \alpha = 0.2, \tilde{T} = 0.5$ .

Next, we consider a system of FODEs each having a different fractional index.

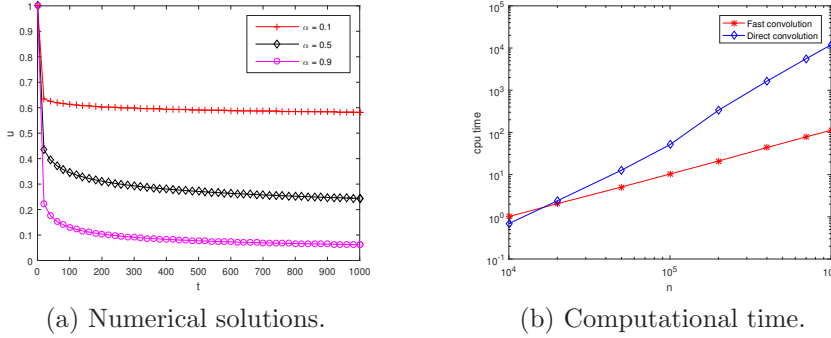


FIG. 7.2. Numerical solutions and the computational time of the two different convolutions for Case II,  $\tau = 0.01, B = 5, N = 64, m = 2, \sigma_k = k\alpha$ .

EXAMPLE 7.2. Consider the following system of equations

$$\begin{cases} {}_C D_{0,t}^{\alpha_1} u(t) = w + (v - c_1)u, \\ {}_C D_{0,t}^{\alpha_2} v(t) = 1 - c_2 v - u^2, \\ {}_C D_{0,t}^{\alpha_3} w(t) = -u - c_3 w, \end{cases} \quad (7.5)$$

where  $0 < \alpha_k \leq 1$  ( $k = 1, 2, 3$ ),  $c_1, c_2$  and  $c_3$  are positive constants,  $c_2 > 1/2$ .

The system (7.5) can be discretized similarly as that of the previous example. Here we always take the memory length  $\Delta T = \tau$ . Let  $U_n, V_n$  and  $W_n$  be the approximate solutions of  $u(t_n), v(t_n)$  and  $w(t_n)$ , respectively. Then the fully discrete scheme for the system (7.5) is given by:

$$\begin{cases} L_{\tau}^{(-\alpha_1, n, 2, m)}(U - U_0) + H_{\tau, \tau}^{(-\alpha_1, n, m)}(U - U_0) = W_n + (V_n - c_1)U_n, \\ L_{\tau}^{(-\alpha_2, n, 2, m)}(V - V_0) + H_{\tau, \tau}^{(-\alpha_2, n, m)}(V - V_0) = 1 - c_2 V_n - U_n^2, \\ L_{\tau}^{(-\alpha_3, n, 2, m)}(W - W_0) + H_{\tau, \tau}^{(-\alpha_3, n, m)}(W - W_0) = -U_n - c_3 W_n, \end{cases} \quad (7.6)$$

where  $n \geq 3$ ,  $L_{\tau}^{(-\alpha, n, 2, m)}$  and  $H_{\tau, \tau}^{(-\alpha, n, m)}$  ( $\alpha = \alpha_k, k = 1, 2, 3$ ) are defined by (4.1) and (5.3), respectively. Here  $m$  is the number of correction terms. Because we use quadratic interpolation,  $U_k, V_k, W_k$  for  $k = 1, 2$  need to be known, which can be derived using the known methods with smaller stepsize. Here we use the second-order generalized Newton-Gregory formula (see [19]) with one correction term and smaller stepsize  $\tau^2$  to derive these values.

Similar to the previous example, we also take the basis  $B = 5$  and the number of quadrature points  $N = 64$  when (5.3) is used.

If  $\alpha_1 = \alpha_2 = \alpha_3 = \alpha$ , then (7.5) is just the fractional Lorenz system [31]. It has been proved that the fractional Lorenz system (7.5) is dissipative [31] and has an absorbing set defined by a ball  $B(0, \sqrt{a/b} + \epsilon)$ , where  $a = 1/2$  and  $b = \min\{c_1, c_2 - 1/2, c_3\}$ . We take  $c_1 = 1/4, c_2 = 1, c_3 = 1/4$  and the initial conditions as those in [31], i.e.,  $U_0 = u(0) = 2, V_0 = v(0) = 0.9, W_0 = w(0) = 0.2$ , the time stepsize is taken as  $\tau = 0.01$ . We compute numerical solutions for  $t \in [0, 1000]$ , which is much larger than that in [31]. Numerical solutions for  $\alpha = 0.9$  are shown in Figure 7.3. We can easily find that  $U_n^2 + V_n^2 + W_n^2 < 2$ , which means  $(U_n, V_n, W_n) \in B(0, \sqrt{2})$ . For other fractional orders  $\alpha_k = \alpha$ , we have similar results, see also [31]. Next, we

choose different  $\alpha_1, \alpha_2$ , and  $\alpha_3$ , and exhibit the numerical solutions in Figure 7.4 for  $(\alpha_1, \alpha_2, \alpha_3) = (0.9, 0.8, 0.7)$  and  $(\alpha_1, \alpha_2, \alpha_3) = (0.7, 0.8, 0.9)$ . We can see that the numerical solutions  $(U_n, V_n, W_n)$  are also in a ball. For other choices of the fractional orders, we have similar results, which are not provided here.

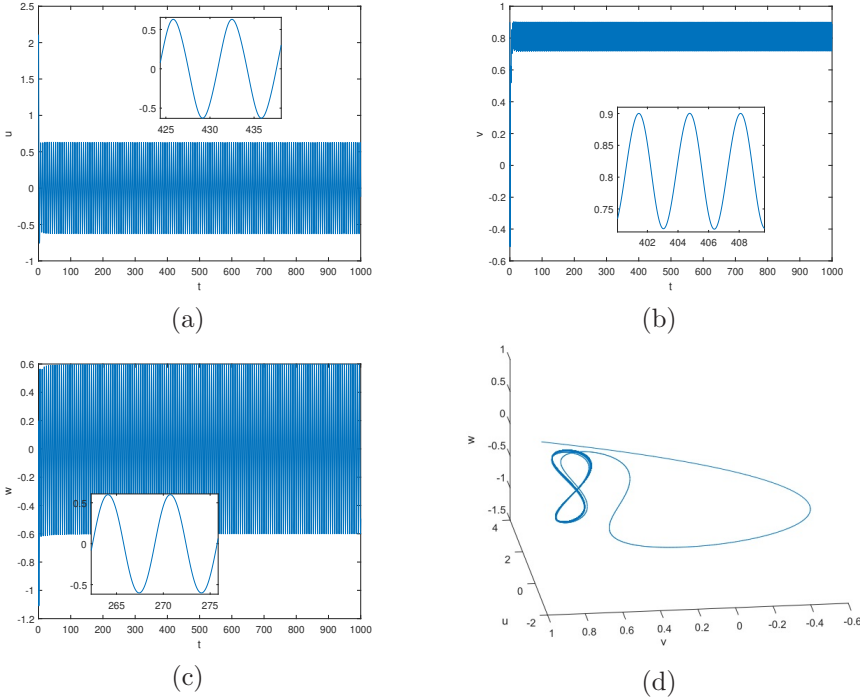


FIG. 7.3. Numerical solutions for Example 7.2,  $\tau = 0.01, m = 2, \sigma_k = k\alpha, \alpha = 0.9$ .

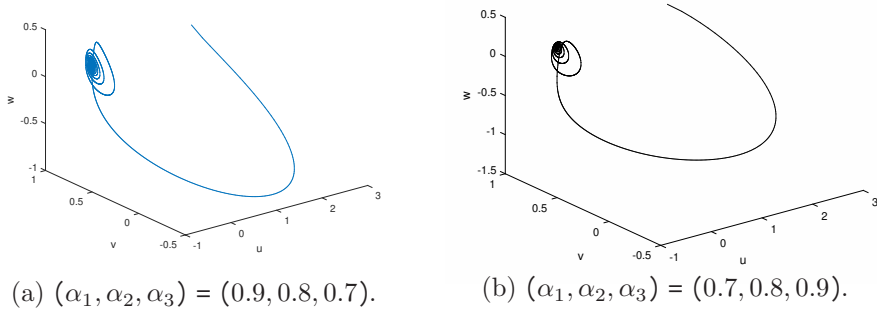


FIG. 7.4. Numerical solutions for Example 7.2,  $t \in [0, 1000]$ ,  $\tau = 0.01, m = 0$ .

EXAMPLE 7.3. Consider the following nonlinear time-fractional PDE

$${}_C D_{0,t}^\alpha u(x, t) = \partial_x^2 u(x, t) + u(x, t)(1 - u^2(x, t)), \quad x \in (0, 1), \quad 0 < \alpha \leq 1 \quad (7.7)$$

subject the homogeneous boundary conditions  $u(0, t) = u(1, t) = 0$  and the initial condition  $u(x, 0) = 2 \sin(2\pi x)$ .

Let  $h = 1/M$  as the stepsize in space, where  $M$  is a positive integer. The time direction is discretized as that in Example 7.1 and the space derivative is discretized by the second-order central difference method. We take  $\Delta T = 0.5$ ,  $\tilde{T} = 1$ ,  $B = 5$ ,  $N = 64$  in (5.3), and  $M = 128$ , and numerical solutions for  $\alpha = 0.1, 0.5, 0.9$  at different time  $t = 100, 500, 1000, 2000, 3000, 4000, 5000$  are shown in Figures 7.5(a)–(c). As the fractional order  $\alpha$  increases, the solution decays faster as  $t$  evolves. Figure 7.5(d) gives the ratio of the computational time of the direct convolution method and the fast convolution method, and shows that the fast method is much faster. Since the fast method uses much less memory, hence, the computational time is reduced significantly. in fact, at the final time  $t = 5000$ , the fast method took about 9 minutes, but the direct method took about 43 hours.

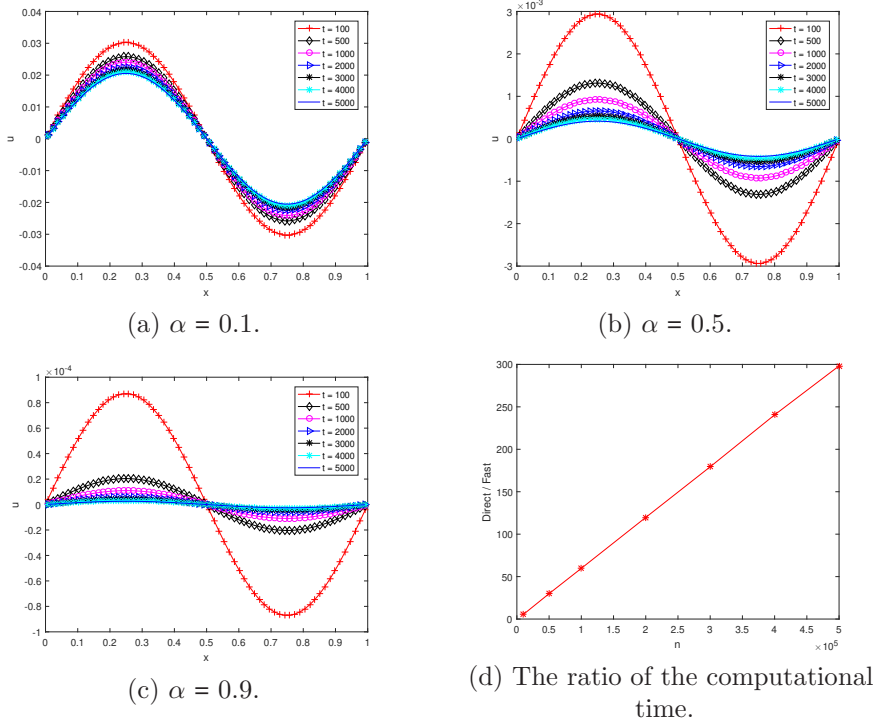


FIG. 7.5. Numerical solutions and computational cost for Example 7.3,  $\tau = 0.01$ ,  $m = 2$ ,  $\sigma_k = k\alpha$ .

**8. Conclusion and discussion.** In this paper, we propose a stable fast memory-saving time-stepping method for both fractional integral and derivative operators, which is applied to solve FDEs. We generalize the fast convolution in [20] for fractional operators, while we use the (truncated) Gauss–Laguerre quadrature to discretize the kernel in the fractional operators instead of the trapezoidal rule in [20] and the Gauss–Legendre quadrature in [14, 16]. We also introduced correction terms in our fast method such that the non-smooth solutions of the FDEs can be resolved accurately. Our fast method has  $O(n_0 + \kappa(N) \log(n_T - n_0))$  active memory and  $O(n_0 n_T + \kappa(N) (n_T - n_0) \log(n_T - n_0))$  operations when it is applied to solve FDEs, where  $n_0 = \Delta T / \tau$ ,  $n_T = T / \tau$ ,  $\tau$  is the stepsize,  $T$  is the final time, and  $\kappa(N)$  is the number of quadrature points in the truncated Gauss–Laguerre quadrature. If the memory length  $\Delta T = \tau$ , then the complexity is the same as that in [20]. If we choose

a suitable memory length  $\Delta T$  and  $N$ , then the present fast method is similar to that in [14, 16], that is, the kernel  $k_\alpha(t)$  is approximated via the truncated Gauss–Laguerre quadrature for all  $t \in [\Delta T, T]$ . In this case, the memory and computational cost of our method are  $O(n_0 + \kappa(N))$  and  $O(n_0 n_T + \kappa(N)(n_T - n_0))$ , respectively, which was also verified by numerical simulations, see Example 7.1.

Compared with the fast convolution in [20], a much larger basis  $B$  can be applied in our fast method. We also present a criteria on how to choose the basis  $B$  such that the desired accuracy can be derived.

We considered the fast method for the fractional derivative of any order and fractional integral of order  $\alpha \in [0, 1]$ . In fact, our method can be extended to the fractional integral of order greater than 1. For example, for  $\alpha \in [1, 2]$ , Eq. (3.4) still holds in the sense that the finite part integral Eq. (3.4) is equivalent to

$$k_\alpha(t) = \frac{t}{\Gamma(\alpha)\Gamma(2-\alpha)} \int_0^\infty \lambda^{1-\alpha} e^{-t\lambda} d\lambda.$$

Thus, the fast method for a fractional integral of order  $\alpha \in [1, 2]$  can be derived by using the present algorithm. In the future, we will apply the fast method to solve a large system of time-fractional PDEs, perhaps in three spacial dimensions. We will also explore how to efficiently calculate the discrete convolution  $\sum_{k=0}^n \omega_{n-k} u(t_k)$ , where the quadrature weights  $\{\omega_n\}$  are not from the interpolation as done in the present work, but from the generating functions, see, e.g., [19].

## REFERENCES

- [1] D. BAFFET AND J. S. HESTHAVEN, *A kernel compression scheme for fractional differential equations*, SIAM J. Numer. Anal., 55 (2017), pp. 496–520.
- [2] W. CAO, F. ZENG, Z. ZHANG, AND G. E. KARNIADAKIS, *Implicit-explicit difference schemes for nonlinear fractional differential equations with nonsmooth solutions*, SIAM J. Sci. Comput., 38 (2016), pp. A3070–A3093.
- [3] X. CHEN, F. ZENG, AND G. E. KARNIADAKIS, *A tunable finite difference method for fractional differential equations with non-smooth solutions*, Comput. Methods Appl. Mech. Engrg., 318 (2017), pp. 193–214.
- [4] L. D’AMORE, A. MURLI, AND M. RIZZARDI, *An extension of the Henrici formula for Laplace transform inversion*, Inverse Problems, 16 (2000), pp. 1441–1456.
- [5] W. DENG, *Short memory principle and a predictor-corrector approach for fractional differential equations*, J. Comput. Appl. Math., 206 (2007), pp. 174–188.
- [6] K. DIETHELM, *Generalized compound quadrature formulae for finite-part integrals*, IMA J. Numer. Anal., 17 (1997), pp. 479–493.
- [7] ———, *The analysis of fractional differential equations*, Springer-Verlag, Berlin, 2010.
- [8] K. DIETHELM, J. M. FORD, N. J. FORD, AND M. WEILBEER, *Pitfalls in fast numerical solvers for fractional differential equations*, J. Comput. Appl. Math., 186 (2006), pp. 482–503.
- [9] K. DIETHELM, N. J. FORD, AND A. D. FREED, *Detailed error analysis for a fractional Adams method*, Numer. Algorithms, 36 (2004), pp. 31–52.
- [10] N. J. FORD AND A. C. SIMPSON, *The numerical solution of fractional differential equations: Speed versus accuracy*, Numerical Algorithms, 26 (2001), pp. 333–346.
- [11] L. GALEONE AND R. GARRAPPA, *Fractional Adams–Moulton methods*, Math. Comput. Simulation, 79 (2008), pp. 1358–1367.
- [12] G.-H. GAO, Z.-Z. SUN, AND H.-W. ZHANG, *A new fractional numerical differentiation formula to approximate the Caputo fractional derivative and its applications*, J. Comput. Phys., 259 (2014), pp. 33–50.
- [13] J. JIA AND H. WANG, *A fast finite volume method for conservative space-fractional diffusion equations in convex domains*, J. Comput. Phys., 310 (2016), pp. 63–84.
- [14] S. JIANG, J. ZHANG, Q. ZHANG, AND Z. ZHANG, *Fast evaluation of the Caputo fractional derivative and its applications to fractional diffusion equations*, Commun. Comput. Phys., 21 (2017), pp. 650–678.

[15] C. LI AND F. ZENG, *Numerical methods for fractional calculus*, CRC Press, Boca Raton, FL, 2015.

[16] J.-R. LI, *A fast time stepping method for evaluating fractional integrals*, SIAM J. Sci. Comput., 31 (2010), pp. 4696–4714.

[17] Z. LI, Z. LIANG, AND Y. YAN, *High-order numerical methods for solving time fractional partial differential equations*, J. Sci. Comput., (2017), pp. 1–19.

[18] M. LÓPEZ-FERNÁNDEZ, C. LUBICH, AND A. SCHÄDLE, *Adaptive, fast, and oblivious convolution in evolution equations with memory*, SIAM J. Sci. Comput., 30 (2008), pp. 1015–1037.

[19] C. LUBICH, *Discretized fractional calculus*, SIAM J. Math. Anal., 17 (1986), pp. 704–719.

[20] C. LUBICH AND A. SCHÄDLE, *Fast convolution for nonreflecting boundary conditions*, SIAM J. Sci. Comput., 24 (2002), pp. 161–182.

[21] C. LV AND C. XU, *Error analysis of a high order method for time-fractional diffusion equations*, SIAM J. Sci. Comput., 38 (2016), pp. A2699–A2724.

[22] G. MASTROIANNI AND G. MONEGATO, *Truncated quadrature rules over  $(0, \infty)$  and Nyström-type methods*, SIAM J. Numer. Anal., 41 (2003), pp. 1870–1892.

[23] W. MCLEAN, *Fast summation by interval clustering for an evolution equation with memory*, SIAM J. Sci. Comput., 34 (2012), pp. A3039–A3056.

[24] R. METZLER AND J. KLAFTER, *The random walk’s guide to anomalous diffusion: a fractional dynamics approach*, Phys. Rep., 339 (2000), pp. 1–77.

[25] H.-K. PANG AND H.-W. SUN, *Fast numerical contour integral method for fractional diffusion equations*, J. Sci. Comput., 66 (2016), pp. 41–66.

[26] I. PODLUBNY, *Fractional differential equations*, Academic Press, Inc., San Diego, CA, 1999.

[27] S. G. SAMKO, A. A. KILBAS, AND O. I. MARICHEV, *Fractional integrals and derivatives: Theory and applications*, Gordon and Breach Science Publishers, Yverdon, 1993.

[28] A. SCHÄDLE, M. LÓPEZ-FERNÁNDEZ, AND C. LUBICH, *Fast and oblivious convolution quadrature*, SIAM J. Sci. Comput., 28 (2006), pp. 421–438.

[29] Z.-Z. SUN AND X. WU, *A fully discrete difference scheme for a diffusion-wave system*, Appl. Numer. Math., 56 (2006), pp. 193–209.

[30] C.-L. WANG, Z.-Q. WANG, AND H.-L. JIA, *An hp-version spectral collocation method for nonlinear Volterra integro-differential equation with weakly singular kernels*, J. Sci. Comput., (2017), pp. 1–32.

[31] D. WANG AND A. XIAO, *Dissipativity and contractivity for fractional-order systems*, Nonlinear Dynamics, 80 (2015), pp. 287–294.

[32] H. WANG AND T. S. BASU, *A fast finite difference method for two-dimensional space-fractional diffusion equations*, SIAM J. Sci. Comput., 34 (2012), pp. A2444–A2458.

[33] H. WANG AND N. DU, *Fast alternating-direction finite difference methods for three-dimensional space-fractional diffusion equations*, J. Comput. Phys., 258 (2014), pp. 305–318.

[34] J. A. C. WEIDEMAN, *Optimizing talbots contours for the inversion of the laplace transform*, SIAM Journal on Numerical Analysis, 44 (2006), pp. 2342–2362.

[35] J. A. C. WEIDEMAN AND L. N. TREFETHEN, *Parabolic and hyperbolic contours for computing the bromwich integral*, Math. Comp., 76 (2007), pp. 1341–1356.

[36] Y. YU, P. PERDIKARIS, AND G. E. KARNIADAKIS, *Fractional modeling of viscoelasticity in 3d cerebral arteries and aneurysms*, J. Comput. Phys., 323 (2016), pp. 219–242.

[37] M. ZAYERNOURI AND A. MATZAVINOS, *Fractional Adams-Bashforth/Moulton methods: An application to the fractional Keller-Segel chemotaxis system*, J. Comput. Phys., 317 (2016), pp. 1–14.

[38] F. ZENG, C. LI, F. LIU, AND I. TURNER, *The use of finite difference/element approaches for solving the time-fractional subdiffusion equation*, SIAM J. Sci. Comput., 35 (2013), pp. A2976–A3000.

[39] ———, *Numerical algorithms for time-fractional subdiffusion equation with second-order accuracy*, SIAM J. Sci. Comput., 37 (2015), pp. A55–A78.

[40] F. ZENG, Z. MAO, AND G. E. KARNIADAKIS, *A generalized spectral collocation method with tunable accuracy for fractional differential equations with end-point singularities*, SIAM J. Sci. Comput., 39 (2017), pp. A360–A383.

[41] F. ZENG, Z. ZHANG, AND G. E. KARNIADAKIS, *Fast difference schemes for solving high-dimensional time-fractional subdiffusion equations*, J. Comput. Phys., 307 (2016), pp. 15–33.

[42] F. ZENG, Z. ZHANG, AND G. E. KARNIADAKIS, *Second-order numerical methods for multi-term fractional differential equations: Smooth and non-smooth solutions*, arXiv:1701.00996, 2017.

[43] L. ZHANG, H.-W. SUN, AND H.-K. PANG, *Fast numerical solution for fractional diffusion equations by exponential quadrature rule*, J. Comput. Phys., 299 (2015), pp. 130–143.